Harmful Algae 63 (2017) 94–108

Contents lists available at ScienceDirect

Harmful Algae

journal homepage: www.elsevier.com/locate/hal

Impacts of the 2014 severe drought on the *Microcystis* bloom in San Francisco Estuary

P.W. Lehman[a,*], T. Kurobe[b], S. Lesmeister[c], D. Baxa[b], A. Tung[c], S.J. Teh[b]

[a] Interagency Ecological Program, California Department of Fish and Wildlife, 2109 Arch Airport Road, Stockton, CA, 95206, USA
[b] Department of Anatomy, Physiology and Cell Biology, School of Veterinary Medicine, 1089 Veterinary Medicine Dr., Vet Med 3B, University of California, Davis, CA, 95616, USA
[c] Division of Environmental Services, California Department of Water Resources, 3500 Industrial Blvd., West Sacramento, CA, 95691, USA

ARTICLE INFO

Article history:
Received 2 July 2016
Received in revised form 21 January 2017
Accepted 29 January 2017
Available online 17 February 2017

Keywords:
Microcystis
Drought
Microcystins
Cyanobacteria
Climate
Water quality
qPCR

ABSTRACT

The increased frequency and intensity of drought with climate change may cause an increase in the magnitude and toxicity of freshwater cyanobacteria harmful algal blooms (CHABs), including *Microcystis* blooms, in San Francisco Estuary, California. As the fourth driest year on record in San Francisco Estuary, the 2014 drought provided an opportunity to directly test the impact of severe drought on cyanobacteria blooms in SFE. A field sampling program was conducted between July and December 2014 to sample a suite of physical, chemical, and biological variables at 10 stations in the freshwater and brackish reaches of the estuary. The 2014 *Microcystis* bloom had the highest biomass and toxin concentration, earliest initiation, and the longest duration, since the blooms began in 1999. Median chlorophyll *a* concentration increased by 9 and 12 times over previous dry and wet years, respectively. Total microcystin concentration also exceeded that in previous dry and wet years by a factor of 11 and 65, respectively. Cell abundance determined by quantitative PCR indicated the bloom contained multiple potentially toxic cyanobacteria species, toxic *Microcystis* and relatively high total cyanobacteria abundance. The bloom was associated with extreme nutrient concentrations, including a 20-year high in soluble reactive phosphorus concentration and low to below detection levels of ammonium. Stable isotope analysis suggested the bloom varied with both inorganic and organic nutrient concentration, and used ammonium as the primary nitrogen source. Water temperature was a primary controlling factor for the bloom and was positively correlated with the increase in both total and toxic *Microcystis* abundance. In addition, the early initiation and persistence of warm water temperature coincided with the increased intensity and duration of the *Microcystis* bloom from the usual 3 to 4 months to 8 months. Long residence time was also a primary factor controlling the magnitude and persistence of the bloom, and was created by a 66% to 85% reduction in both the water inflow and diversion of water for agriculture during the summer. We concluded that severe drought conditions can lead to a significant increase in the abundance of *Microcystis* and other cyanobacteria, as well as their associated toxins.

1. Introduction

Harmful cyanobacteria blooms (CHABs) are expected to increase worldwide with the frequency and intensity of drought conditions produced by either anthropogenic or climatic conditions (IPCC, 2007; Elliott, 2012; O'Neil et al., 2012; Paerl and Paul, 2012; Paerl and Scott, 2010). Increased water temperature, salinization, duration of the summer season, water stratification, evaporation and hydraulic residence time, associated with drought conditions, are expected to favor development of freshwater CHABS, particularly *Microcystis*, the most cosmopolitan freshwater CHAB worldwide (Van Gremberghe et al., 2011; Mosley, 2015). *Microcystis* can cause a harmful algal bloom, because it often contains hepatotoxic microcystins, which promote liver cancer in humans and wildlife across ecosystems, (Zegura et al., 2003; International Agency for Research on Cancer, 2006; Ibelings and Havens, 2008; Miller et al., 2010), and lipopolysaccharide endotoxins, which inhibit ion transport in fish gills, as well as fish embryo development (Codd, 2000). The potential of *Microcystis* blooms to increase during drought is greater than for most freshwater CHABs, because its tolerance of salinity enables it to survive and expand into brackish and marine water environments

* Corresponding author.
E-mail address: Peggy.Lehman@water.ca.gov (P.W. Lehman).

http://dx.doi.org/10.1016/j.hal.2017.01.011

(Paerl, 1988; Sellner et al., 1988; Rocha et al., 2002; Robson and Hamilton, 2003). In addition, *Microcystis* out-competes phytoplankton and other cyanobacteria at elevated water temperature, a common condition during drought (Paerl and Paul, 2012). However, relatively little is known about how *Microcystis* varies directly with severe drought conditions.

Microcystis spp. (*Microcystis*) blooms have occurred yearly in San Francisco Estuary (SFE) since 1999 (Lehman et al., 2005, 2013). The bloom occurs over a four month period and peaks in the summer during August and September. On average, about 20% of the cells during *Microcystis* blooms in SFE contain microcystins, which occur in *Microcystis* colonies, dissolved in the water column and aquatic animal tissue (Lehman et al., 2005, 2013; Baxa et al., 2010). *Microcystis* grows well in SFE where nutrients are in excess (Jassby, 2008). Both isotope and nitrogen uptake studies indicated *Microcystis* rapidly took up ammonium, which was the primary nitrogen source for the bloom (Lee et al., 2015; Lehman et al., 2015). Conditions characteristic of drought, warm water temperature and low streamflow, were correlated with the increase in *Microcystis* biomass and toxin content (Lehman et al., 2008, 2013). Although some data are available on the variation of *Microcystis* blooms with wet and dry conditions in SFE, no data are available on the impact of severe drought conditions on the amplitude, toxin content, duration or causal factors associated with *Microcystis* blooms. Because 2014 was the fourth largest drought year on record in California, information on the *Microcystis* bloom amplitude, toxin content and controlling factors in 2014 provided an opportunity to gain insight into the potential impact of future severe climate or anthropogenic induced droughts on CHABS in SFE, needed to develop management strategies.

The purpose of this study was to characterize the amplitude, species composition and toxin concentration of the *Microcystis* bloom in SFE and its association with environmental conditions during the severe drought of 2014. The study addressed the hypotheses that during severe drought conditions the *Microcystis* bloom biomass and toxin concentration will 1) increase significantly and 2) be controlled by similar environmental factors, compared with previous wet and dry conditions. These hypotheses were evaluated by comparing the *Microcystis* bloom and associated conditions during the 2014 severe drought with two previous wet (2004–2005) and dry (2007–2008) years. Information on the impacts of drought on *Microcystis* blooms is critically needed to develop strategies for managing CHABs in the highly urbanized SFE. Here drought impacts from both climate change and water management affect the quantity and quality of water used for drinking, agriculture, recreation, industry and urbanization of over 25 million people, as well as habitat needed for threatened and endangered estuarine fish species (Sommer et al., 2007).

2. Materials and methods

2.1. Site description

SFE is the largest estuary on the west coast of North America and is located in central California, USA. The estuary contains an inland delta of 2990 km^2 with 1100 km of waterways, is bounded by the Sacramento River on the north and the San Joaquin River on the south, and is commonly referred to as the Sacramento-San Joaquin Delta (Delta; Fig. 1). The Delta extends upstream to the head of the tide at Freeport on the Sacramento River and Vernalis on the San Joaquin River. Water from these two major rivers converge near Antioch and flow into a chain of downstream marine bays – Suisun, San Pablo and San Francisco. The water year 2014 was the fourth driest year on record in SFE (http://www.water.ca.

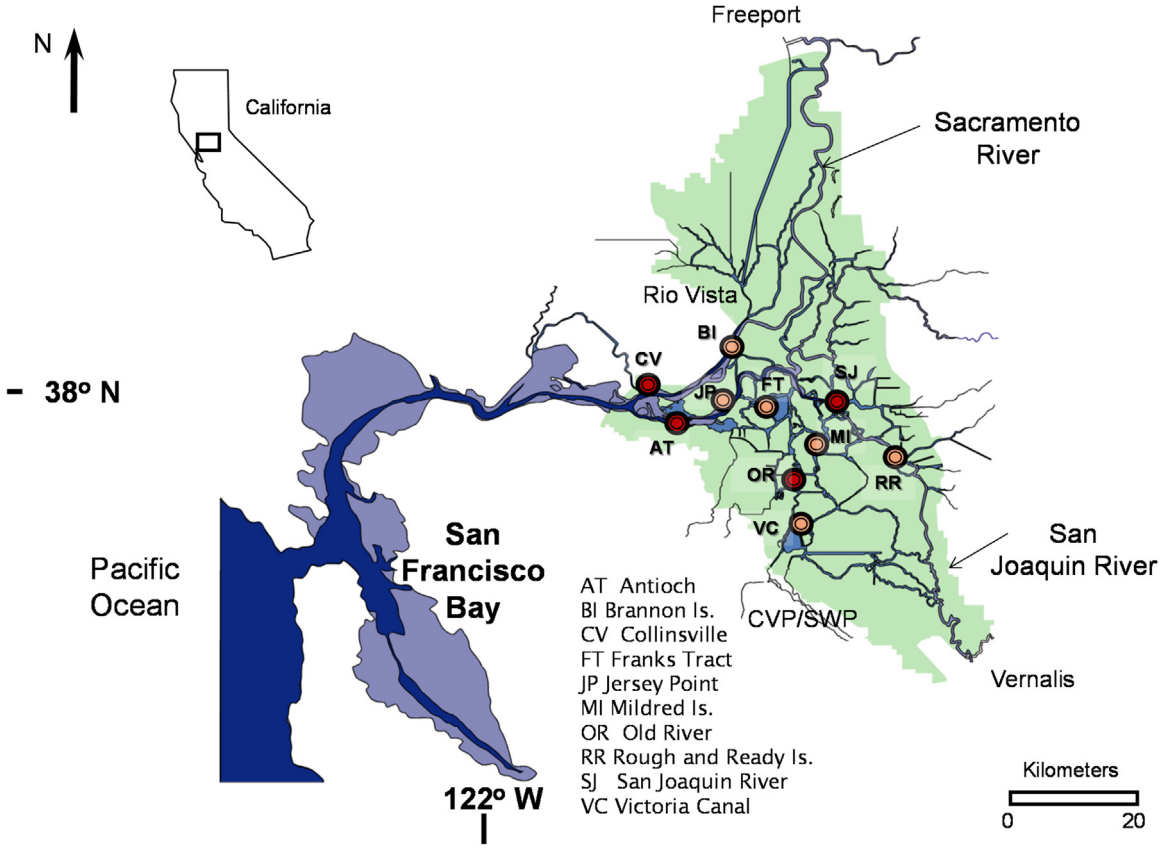

Fig. 1. Map of the estuary showing the location of the sampling stations.

gov/dayflow/output). Streamflow during the peak of the *Microcystis* bloom in August and September of 2014 reached 238 ± 18 $m^3 s^{-1}$ and 302 ± 1 $m^3 s^{-1}$ for the Sacramento and San Joaquin Rivers, respectively. An important feature of the Delta hydrology is the large quantity of water diverted for agriculture from the southern portion of the delta that can cause net negative streamflow in the lower San Joaquin River. Net negative streamflow allows water from the Sacramento River to enter the San Joaquin River at the confluence of the two rivers (Lehman et al., 2008, 2015). Water depth varies from a few meters in the shallow flooded islands, like Mildred Island, to 13 m in the center of the major river channels. Tides in the delta reach 2 m in height, have velocities up to 30 cm s^{-1} and range 10 km during tidal excursion. Although nitrogen and phosphorus concentrations are in excess, light limitation due to high total suspended solids concentration limits development of eutrophic conditions (Jassby, 2008).

2.2. Field sampling

Sampling was conducted bi-weekly at 10 stations (n = 120) between July and December 2014 in the San Joaquin River, from Antioch to Stockton, and in the Sacramento River, from Brannon Island to Collinsville (Fig. 1). *Microcystis* colonies and associated phytoplankton, cyanobacteria and organic material greater than 75 μm in diameter were gently collected from the surface of the water column by a hand tow of a 0.3 m diameter plankton net (75 μm mesh) over a distance of 30.5 m in 2014, and with a 1 to 3 min slow moving tow in previous years (Lehman et al., 2013). The net was fitted with floats that kept the ring just below the surface, making the net tow an integrated sample of the 0.3 m surface layer. A surface net tow was used in order to get a representative sample of the large *Microcystis* colonies, which were often widely dispersed across the surface of the water column and can reach 50,000 μm in diameter. The large mesh used for the net tow also reduced clogging from the heavy suspended sediment, which characterizes SFE. *Microcystis* biomass and chlorophyll *a* concentrations in the net tow were corrected to the total volume of water sampled using a General Oceanics 2030R flow meter. Subsurface water for measurement of microcystin, nutrient, total and dissolved organic carbon, total and volatile suspended solids concentration, as well as phytoplankton and cyanobacteria taxonomic biovolume and composition was collected by a 3-L van Dorn bottle at 0.3 m. Water samples for all water quality analyses were stored on ice after collection and processed within 1 to 3 h.

Water temperature, pH, specific conductance, turbidity (NTU), and dissolved oxygen concentration were also measured at 0.3 m depth using a Yellow Springs Instrument (YSI) 6600 water quality sonde. Surface irradiance and light attenuation within the photic zone were measured by a Li-COR spherical quantum sensor LI-193. Areal light levels within the euphotic zone were computed by integrating light levels to the depth of 1% light using the trapezoid rule. Long-term continuous (15 min interval) and discrete (bi-weekly to monthly) water quality data used in the historical data analysis were collected by the California Department of Water Resources and U. S. Bureau of Reclamation (http//www.water.ca.gov/iep/products/data). Streamflow and agricultural diversion data were obtained from the DAYFLOW database (http://www.water.ca.gov/dayflow/output).

2.3. Water quality analyses

Water for chloride, ammonium, nitrate plus nitrite, silica and soluble reactive phosphorus (SRP) analysis was filtered through nucleopore filters (0.45 μm pore size) and frozen until analysis (American Public Health Association et al., 1998; United States Environmental Protection Agency, 1983; United States Geological Survey, 1985). Water for dissolved organic carbon analysis was filtered through a pre-combusted GF/F filter (pore size 0.7 μm) and kept at 4 °C until analysis (American Public Health Association et al., 1998). Unfiltered water samples for total and volatile suspended solids, total organic carbon and total phosphate analyses were kept at 4 °C until analysis (American Public Health Association et al., 1998).

Replicate water samples for chlorophyll *a* and phaeophytin pigment analysis were filtered through GF/F filters in the field. Filters were treated with 1% magnesium carbonate solution to prevent acidity, and frozen until analysis. Pigments were extracted in 90% acetone and quantified using spectrophotometry (American Public Health Association et al., 1998).

2.4. Phytoplankton and cyanobacteria composition

Net tow samples for determination of *Microcystis* biovolume (>75 μm size fraction) were preserved with Lugol's solution. The biovolume of *Microcystis* colonies was computed using area based

Table 1
Quantitative real-time polymerase chain reaction (qPCR) assays and their associated primers and probe sequences used to quantify the abundance of *Dolichospermum*, *Aphanizomenon*, *Microcystis* and total cyanobacteria.

Target	Primer/Probe	Sequence (5′-3′)	Standard curve	Efficiency (%)	R^2 value	Reference
Dolichospermum 16S rDNA	DOLIC_SW1105_F526	AGA GTC TGG CTC AAC CAG ATC AA				
	DOLIC_SW1105_R617	ATT TCA CCG CTA CAC CAG GAA TT	y = −3.3094× + 39.983	100.5	0.9997	This study
	DOLIC_SW1105_P566*	CAA AGC TAG AGT ATG GTC GG				
Aphanizomenon 16S rDNA	APHA_SW1101_F524	TAA AGA GTT TGG CTC AAC CAA ATA AG				
	APHA_SW1101_R615	ATT TCA CCG CTA CAC CAG GAA TT	y = −3.271× + 39.090	102.2	0.9991	This study
	APHA_SW1101_P565*	AAA GCT AGA GTG TGG TCG G				
Microcystis 16S rDNA	MIC_SW1109_F499	CGC AGG TGG TCA GCC AA				
	MIC_SW1109_R584	CCT ACT GCT CTC TAG TCT GCC AGT TT	y = −3.4317× + 40.824	95.6	0.9992	This study
	MIC_SW1109_P524*	TCA AAT CAG GTT GCT TAA CGA				
Microcystis mcyD gene	mcyD_F	GGT TCG CCT GGT CAA AGT AA				Rinta-Kanto et al. (2005)
	mcyD_R	CCT CGC TAA AGA AGG GTT GA	y = −3.4801× + 40.389	93.8	0.9986	
	mcyD_P*	ATG CTC TAA TGC AGC AAC GGC AA A				
Cyanobacteria 16S rDNA	CYA16S_F	TCG CCC ATT GCG GAA A				
	CYA16S_R	AGA CAC GGC CCA GAC TCC TA	y = −3.2087× + 40.749	105.0	0.9945	Baxa et al. (2010)
	CYA16S_P*	TTC CCC ACT GCT GCC				

*The probes were labeled with 6FAM and MGBNFQ as reporter and quencher, respectively.

diameter (ABD) with a FlowCAM digital imaging flow cytometer (Fluid Imaging Technologies; Sieracki et al., 1998). In order to more easily measure the biovolume of the colonies, the samples were size fractionated into <300 μm and >300 μm diameter size fractions and read at a magnification of 10× and 4×, respectively. Cell abundance estimates based on FlowCAM measurements were closely correlated with those determined by microscopic analyses ($r = 0.88$, $p < 0.01$).

Whole water (unpreserved) samples collected from 0.3 m depth were used to determine phytoplankton and cyanobacteria biovolume and taxonomic composition (>10 μm size fraction) in sub-surface water. These samples were kept at 4 °C and processed live within 1 to 3 h with a FlowCAM digital imaging flow cytometer. The FlowCAM was fitted with a fluorescence trigger to isolate live phytoplankton from detritus (Sieracki et al., 1998). Digital images of cells were obtained by passing samples through a 100 μl flow cell for 10 min at 10 x magnification.

2.5. Microcystin concentration

The microcystin concentration (microcystin-LR equivalents) in particulate (algal cells) and dissolved fractions (water) was determined for subsurface water using a protein phosphatase inhibition assay (PPIA) kit (Product No. 520032, ABRAXIS, Warminser, PA). Particulate and dissolved fractions were separated by filtering the whole water sample through a glass fiber membrane (934-AH, 0.45 μm pore size, Whatman). Particulate organic matter on the filter was subjected to microcystin extraction using 80% methanol, followed by dilution before quantification of microcystin in the algal fraction by PPIA. The filtrate was used directly for PPIA analysis.

2.6. Quantitative polymerase chain reaction (qPCR) analysis

A qPCR analysis of whole water samples from 0.3 m depth was used to quantify the toxic cyanobacteria in all size fractions within the water column. Subsurface water samples (200–300 ml) for qPCR analysis were filtered through nitrocellulose membrane filters (pore size 0.45 μm) and the filter was used for DNA extraction using a NucleoSpin Plant II Kit (Macherey-Nagel, Bethlehem, Pennsylvania). The qPCR assays were used to quantify the gene targets: 16S ribosomal RNA genes (16S rDNA) for *Dolichospermum*, *Aphanizomenon*, *Microcystis*, and total cyanobacteria, and the microcystin synthetase gene (*mcyD*) for toxin-producing *Microcystis* (Table 1). The qPCR assay for total cyanobacteria was developed against the conserved region of three cyanobacterial genera: *Microcystis*, *Dolichospermum*, and *Nostoc*. The assay also reacts with a wide range of cyanobacteria including *Aphanizomenon*, *Planktothrix*, and *Cylindrospermum*. The copy numbers of 16S rDNA gene were divided by the number of 16S rDNA per genome to obtain the equivalent cell number: *Microcystis aeruginosa* (2 copies, GenBank accession number: AP009552.1), *Dolichospermum* (4 copies, CP003659.1), and *Aphanizomenon* (6 copies, NZ_AZYY00000000.1). For total cyanobacteria, the number of cell equivalents was calculated by dividing the 16S rDNA copy number by 2 because *Microcystis* was the dominant species in SFE (Lehman et al., 2005; Baxa et al., 2010). For toxin producing *Microcystis*, the number of *mcy*D gene copy numbers were directly utilized as the number of cell equivalents, since there is only one copy of *mcy*D gene per *Microcystis* genome (accession number: AP009552.1).

2.7. Isotope analysis

The $\delta^{15}N$ isotope signal in the particulate organic matter within the *Microcystis* net tow (POM-$\delta^{15}N$) and dissolved nitrate in the water column (NO_3-$\delta^{15}N$) were used to identify the use of nitrate as a nitrogen source to the bloom. Replicate samples for isotopic analysis of particulate organic matter (POM) from the net tow were filtered through pre-combusted GF/F filters, dried in a temperature controlled incubator at 60 °C for 48 h and then stored in a desiccator until analysis. Whole water samples for NO_3-$\delta^{15}N$ analysis were filtered through polyether sulfone membrane filters (pore size 0.22 μm) and the filtrate was kept frozen at −20 °C until analysis. Both glass fiber filters and filtrate were analyzed for ^{15}N isotopes at the University of California at Davis Stable Isotope Facility, according to procedures described at the website http://stableisotopefacility.ucdavis.edu

Table 2
Median and standard deviation of water quality and organic carbon variables measured twice per month at 10 stations in the Delta between July and December 2014 for summer (July-September), fall (October-December) and the bloom season (July-December). Differences between the summer and fall seasons were computed using the Mann-Whitney *U* test and were significant at the 0.05 level or higher (*) or non-significant (ns).

variable	summer	fall	dif	season
euphotic zone light, μmole photons m^{-1} s^{-1}	1063 ± 383	869 ± 450	*	958 ± 387
water temperature, °C	23.2 ± 1.9	17.4 ± 4.3	*	21.5 ± 3.8
dissolved oxygen, mg l^{-1}	8.1 ± 0.7	8.4 ± 0.4	*	8.2 ± 0.5
percent dissolved oxygen, %	94 ± 6	88 ± 6	*	91 ± 6
specific conductance, uS cm^{-1}	771 ± 591	912 ± 700	ns	851 ± 679
turbidity, NTU	6.1 ± 6.2	4.8 ± 6.2	*	5.8 ± 6.5
pH	7.9 ± 0.2	7.6 ± 0.2	*	7.8 ± 0.3
chloride, mg l^{-1}	190 ± 179	215 ± 193	ns	207 ± 181
ammonium, mg l^{-1}	0.02 ± 0.01	0.05 ± 0.04	*	0.03 ± 0.02
nitrate, mg l^{-1}	0.18 ± 0.18	0.47 ± 0.18	*	0.33 ± 0.28
total phosphorus, mg l^{-1}	0.11 ± 0.01	0.10 ± 0.01	*	0.11 ± 0.01
soluble reactive phosphorus, mg l^{-1}	0.08 ± 0.01	0.09 ± 0.01	ns	0.08 ± 0.01
N:P molar ratio	6 ± 4	14 ± 7	*	8.8 ± 5.6
silica, mg l^{-1}	13.6 ± 1.5	16.4 ± 1.8	*	14.5 ± 2.5
total dissolved solids, mg l^{-1}	508 ± 358	527 ± 381	ns	52 ± 372
total suspended solids, mg l^{-1}	6 ± 6	6.0 ± 5.9	ns	6 ± 6
net chlorophyll a, μg l^{-1}	1.88 ± 1.27	0.23 ± 0.25	*	1.06 ± 1.26
phaeophytin, μg l^{-1}	0.07 ± 0.07	0.02 ± 0.02	*	0.04 ± 0.04
dissolved organic carbon, mg l^{-1}	2.9 ± 0.7	2.9 ± 0.7	ns	2.9 ± 0.74
total organic carbon, mg l^{-1}	2.95 ± 0.7	3 ± 0.7	ns	3 ± 0.74
dissolved organic nitrogen, mg l^{-1}	0.3 ± 0.15	0.2 ± 0.15	*	0.3 ± 0.15
volatile suspended solids, mg l^{-1}	2 ± 1.5	1.0 ± 1.5	ns	2 ± 1.5

2.8. Statistical analysis

Due to the lack of normality associated with small sample size, statistical analyses were computed using nonparametric statistics. Data were reported as the median and the median absolute deviation (SAS Institute, 2013). Correlation coefficients were computed using Spearman rank correlation, while single and multiple comparisons were computed using the Mann-Whitney U and Kruskal-Wallis nonparametric tests, respectively (SAS Institute, 2013). Significance of each test was at the 0.05 level or higher. Seasons were classified as summer (July through September) and fall (October through December). Historical comparisons between wet (2004 and 2005), dry (2007 and 2008) and the critically dry 2014 water years were made using data collected during the peak of the bloom in August and September at stations AT, CV, OR and SJ; the only stations collected in the same fashion over all five water years (Lehman et al., 2013). Water year classifications were based on statewide runoff criteria and streamflow data (Jones, 2015).

3. Results

3.1. Water quality conditions

Water quality conditions during the 2014 *Microcystis* bloom (July through December) were characterized by relatively high median water temperature (21.5 °C), pH (7.8) and dissolved oxygen concentration (8.2 mg l^{-1}), with relatively low median specific conductance (851 μS cm^{-1}), salinity (207 mg l^{-1} chloride) and turbidity (5.8 NTU; Table 2). Median nutrient concentrations were non-limiting for ammonium (0.03 mg l^{-1}), nitrate (0.33 mg l^{-1}) and SRP (0.08 mg l^{-1}). However, the median N:P molar ratio of 8.8 was lower than the Redfield N:P Ratio of 16:1, considered to be ideal for primary producers (Redfield, 1958). The median areal euphotic zone light level was 958 ± 387 μmole photons m^{-1} s^{-1} (range 798 to 1444 μmole photons m^{-1} s^{-1}). Among stations, lower ($p < 0.05$) light levels occurred in the euphotic zone for the western Delta at stations BI, CV and AT than the landward stations in the central and southern Delta (Fig. 2).

Between seasons, the summer had higher water temperature; percent dissolved oxygen and pH, and lower dissolved oxygen concentration than the fall (Table 2). In contrast, silica, nitrate and ammonium concentration were higher and associated with lower total phosphorus in the fall compared with the summer. The increase in nitrate and ammonium concentration between the summer and fall shifted the N:P molar ratio from 6 to 14, which was closer to the Redfield N:P molar ratio of 16.

The decrease in turbidity in the fall was not accompanied by a significant decrease in total dissolved solids, total suspended solids, total and dissolved organic carbon, or volatile suspended solids concentration (Table 2). Instead, fall was characterized by a decrease in both chlorophyll *a* and phaeophytin pigment, plus dissolved organic nitrogen. Surface turbidity contrasted with the areal light in the euphotic zone, which was greater in the summer than the fall. Median light levels decreased ($p < 0.05$) between summer and fall from 1063 ± 383 μmol photons m^{-1} s^{-1} to 869 ± 450 μmol photons m^{-1} s^{-1} (Fig. 2).

3.2. Bloom biomass

Median chlorophyll *a* concentrations in surface net tows were variable among stations (Fig. 3). Relatively high surface chlorophyll *a* concentration characterized the southern Delta stations VC, RR and OR in the San Joaquin River, where median chlorophyll *a* concentrations of 2–3 μg l^{-1} were 2 to 3 times higher ($p < 0.05$) than at stations AT, CV and FT in the western and northern Delta. However, there was no consistent geographical pattern.

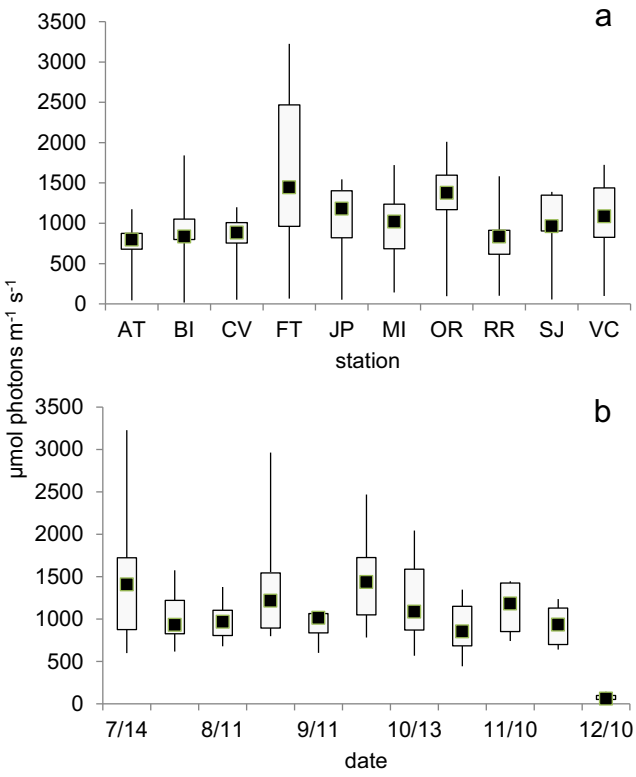

Fig. 2. Median (square), 25th and 75th percentiles (box), maximum and minimum (line) integrated light within the euphotic zone for stations (a) and months (b) between July and December 2014.

Chlorophyll *a* concentration was relatively greater ($p < 0.01$) at BI, the most northerly station sampled on the Sacramento River, than at stations AT and CV, just downstream, and more similar in amplitude to stations on the San Joaquin River. In fact, during August and September, chlorophyll *a* concentration at BI was not significantly different ($p > 0.05$) from stations VC, RR, OR and MI in the central and southern Delta. Among months, median surface chlorophyll *a* concentration was a factor of 8 greater ($p < 0.05$) in the summer during July and September (1.88 μg l^{-1}) than the fall and winter October through December (0.23 μg l^{-1}; Fig. 3).

Microscopic analysis of the >10 μm size fraction indicated *Microcystis* plus other cyanobacteria comprised 83% of the total primary producer biovolume in the subsurface water among stations, with *Microcystis* often comprising 50% or more of the total cyanobacteria (Fig. 4). *Microcystis* and other cyanobacteria biovolume were greater ($p < 0.05$) in the southern Delta at stations OR, RR and VC than other stations. Diatom biovolume comprised the largest percentage (11%) of the remaining primary producer biovolume among stations. Unlike *Microcystis*, diatom, green algae, chrysophyte, cryptophyte, dinoflagellate and flagellate biovolume was greater ($p < 0.05$) in the western Delta at stations BI, CV and AT than other stations.

Among months, *Microcystis* comprised a greater percentage of primary producer biovolume in the subsurface water ($p < 0.05$) during September, compared with July, November and December (Fig. 4). Cryptophytes, dinoflagellates and miscellaneous flagellates characterized ($p < 0.05$) the peak of the bloom in July. In contrast, diatom, green algae and chrysophyte biovolume was greater ($p < 0.01$) during November and December than previous months.

Microcystis colonies in the surface net tow reached a median biovolume of 8×10^9 μm^3 l^{-1}, and were not significantly different among stations (Fig. 5). However, there was a tendency for higher biovolume to occur in the San Joaquin River at stations VC and JP.

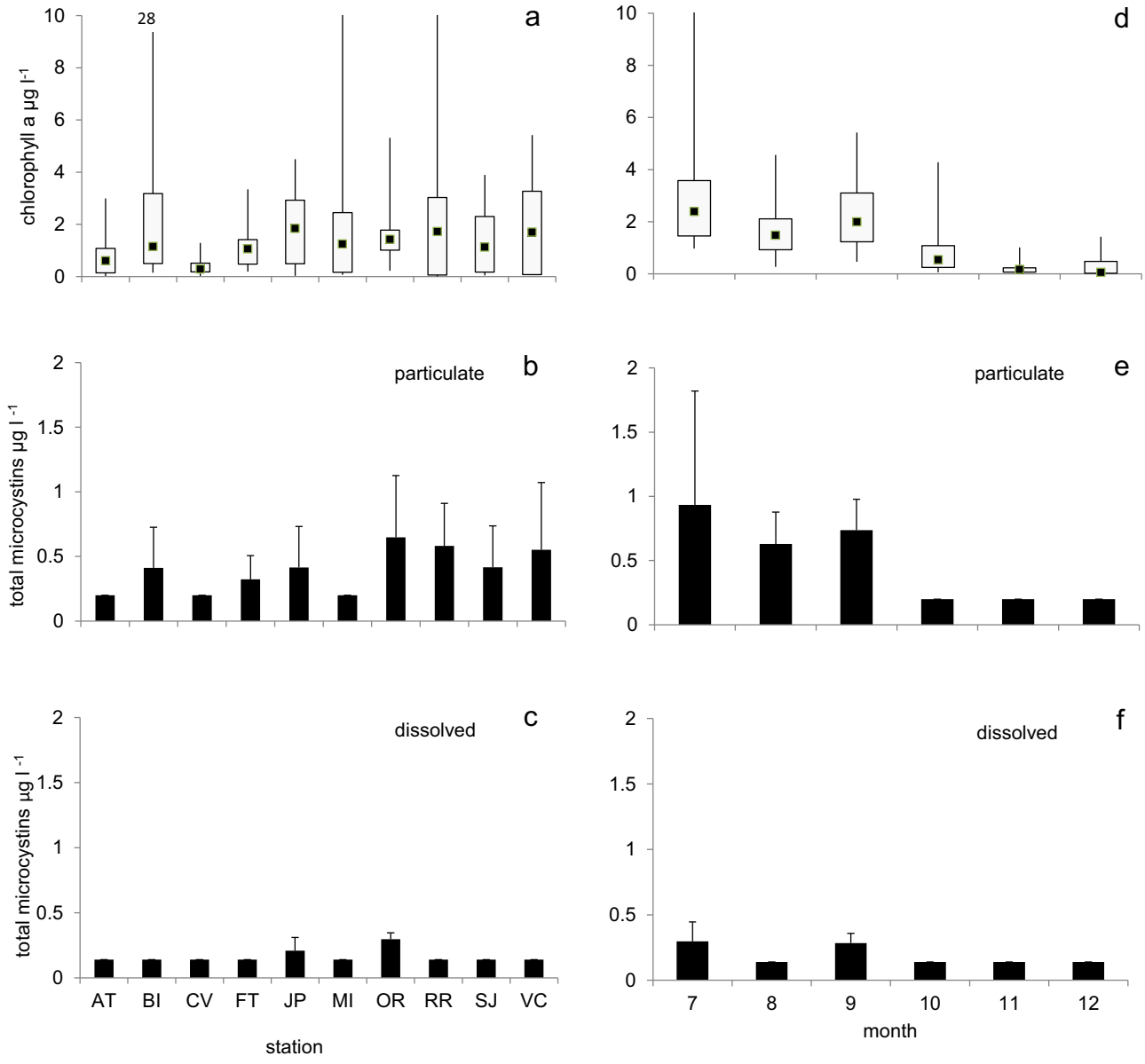

Fig. 3. Median (square), 25th and 75th percentiles (box) and maximum and minimum (line) by station and month for chlorophyll *a* concentration in the surface net tow (a,d), microcystins concentration in the particulate organic matter (b,e) and dissolved in the water column (c,f) for samples taken between July and December 2014.

Among months, the biovolume of the surface colonies decreased successively between July and December ($p < 0.05$).

3.3. Microcystin concentration

Particulate and dissolved microcystin concentration in the subsurface water was highly variable and did not demonstrate a geographic pattern. Median total microcystin concentration (particulate plus dissolved) exceeded the quantification limit of 0.25 $\mu g\,l^{-1}$ in over 50% of the samples and ranged from a median of 0.65 $\mu g\,l^{-1}$ at station OR to less than detection levels at stations AT, CV and MI. There was no statistical difference in the total microcystin concentration among stations, despite elevated concentrations at stations RR (32.9 $\mu g\,l^{-1}$) and MI (11.3 $\mu g\,l^{-1}$) in July (Fig. 3). The dissolved microcystin concentration was usually about six times lower than the particulate microcystin concentration, and also did not differ among stations. In addition, dissolved microcystin concentration was above the limit of quantification for only about 33% of the samples. Both particulate and dissolved microcystin concentrations varied seasonally and were greater ($p < 0.05$) in the summer than the fall.

3.4. Cyanobacteria abundance

Three *Microcystis* species were common in the surface net samples during the bloom, *M. aeruginosa*, *M. flos-aquae* and *M. wesenbergii*. *M. aeruginosa* was the most common species and comprised between 65% and 89% of the total *Microcystis* biovolume (Fig. 6). *M. flos-aquae* comprised the second largest percentage of the total *Microcystis* biovolume and comprised a greater ($p < 0.05$) percentage of the biovolume in the southern Delta at stations RR and VC than other stations. *M. wesenbergii* comprised up to 18% of the total *Microcystis* biovolume and comprised a greater ($p < 0.05$) percentage of the biovolume at stations SJ, MI and BI than other

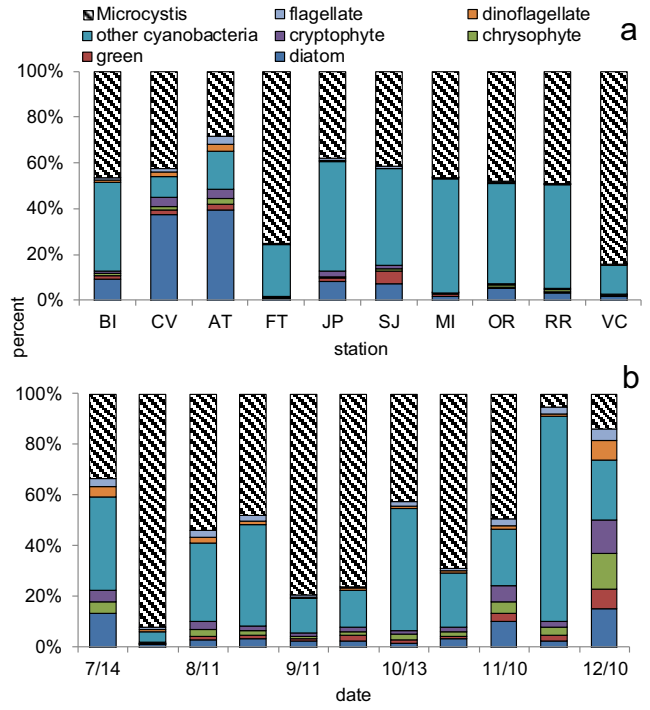

Fig. 4. Percent of total phytoplankton biovolume among taxonomic groups within the >10 μm size fraction and at 0.3 m depth, determined by microscopy among stations (a) and months (b) between July and December 2014.

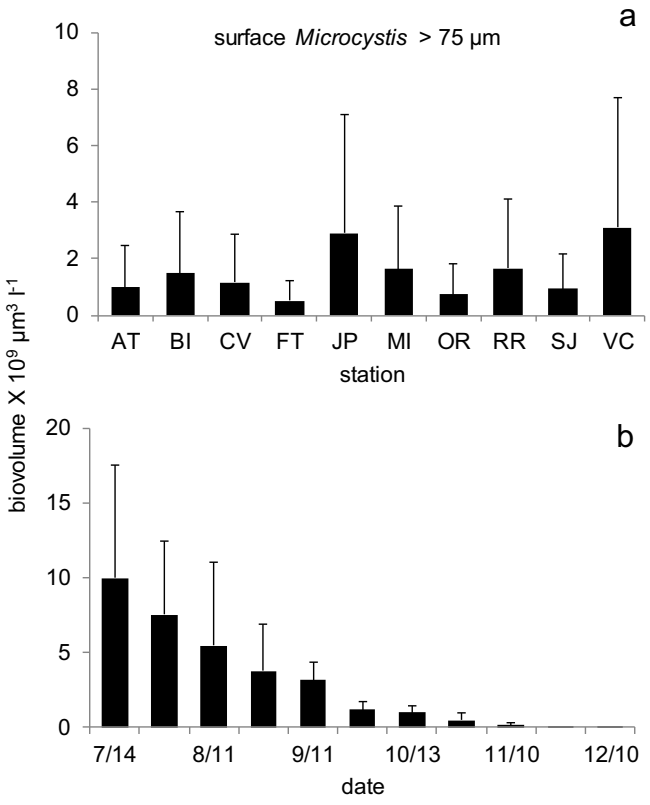

Fig. 5. Median and standard deviation of *Microcystis* biovolume (>75 μm size fraction) in surface net tows among stations (a) and months (b) sampled between July and December 2014.

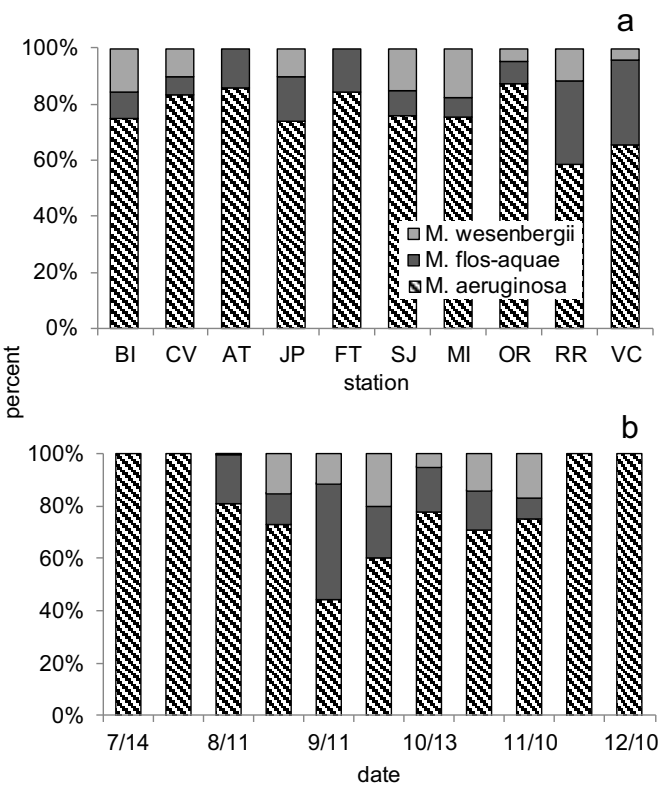

Fig. 6. Percent of *Microcystis* species biovolume in surface net tows (>75 μm size fraction) among stations (a) and months (b) between July and December 2014.

stations. Among months, *M. flos-aquae* and *M. wesenbergii* comprised 40% to 56% of the total *Microcystis* biovolume and had greater ($p < 0.05$) biovolume in September than other months.

The percent abundance of the potentially toxic cyanobacteria genera (qPCR), *Microcystis, Aphanizomenon* and *Dolichospermum,* in the subsurface whole water samples varied among stations. *Microcystis* comprised the largest percentage ($16 \pm 15\%$) of the total cyanobacteria abundance, followed by *Aphanizomenon* spp. ($8 \pm 7\%$) and then *Dolichospermum* spp. (<1%) among stations. However, all three genera combined comprised less than 40% of the total cyanobacteria abundance (Fig. 7a). The greater percent abundance of other cyanobacteria determined by qPCR compared with the percent biovolume determined by microscopy (>10 μm), suggested there were many cyanobacteria in the water column less than 10 μm in diameter (compare Figs. 4 and 7).

There was no significant difference in the percent *Microcystis* or *Dolichospermum* abundance (qPCR) among stations. By contrast, the percent *Aphanizomenon* abundance was greater ($p < 0.05$) in the central and southern Delta (stations FT, JP, OR, SJ, VC, and MI) compared with the western Delta (stations AT and CV). The percent of other cyanobacteria was greater ($p < 0.05$) in the western Delta at station CV compared with the central Delta stations OR, FT or JP, as well as the southern Delta stations RR and MI compared with the central Delta station FT (Fig. 7a).

Total cyanobacteria abundance was greater ($p < 0.05$) in July through September and ranged from 59,495 to 5,749,143 cells ml^{-1} among stations, based on qPCR of subsurface whole water samples. The percent abundance of *Dolichospermum* was greater ($p < 0.05$) in July than other months. The percent *Microcystis* abundance was similarly greater ($p < 0.05$) in the summer, but during August and September (Fig. 7b). In contrast, the percent *Aphanizomenon* abundance was greater in November.

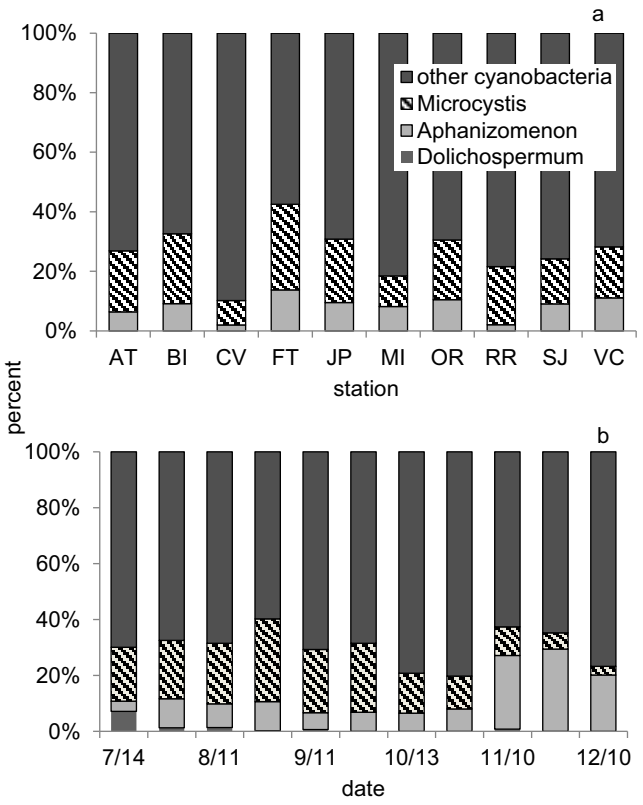

Fig. 7. Percent abundance of *Microcystis*, *Dolichospermum*, *Aphanizomenon* and other cyanobacteria of the total cyanobacteria abundance at all size fractions in whole water samples measured by qPCR analysis among stations (a) and months (b) between July and December 2014.

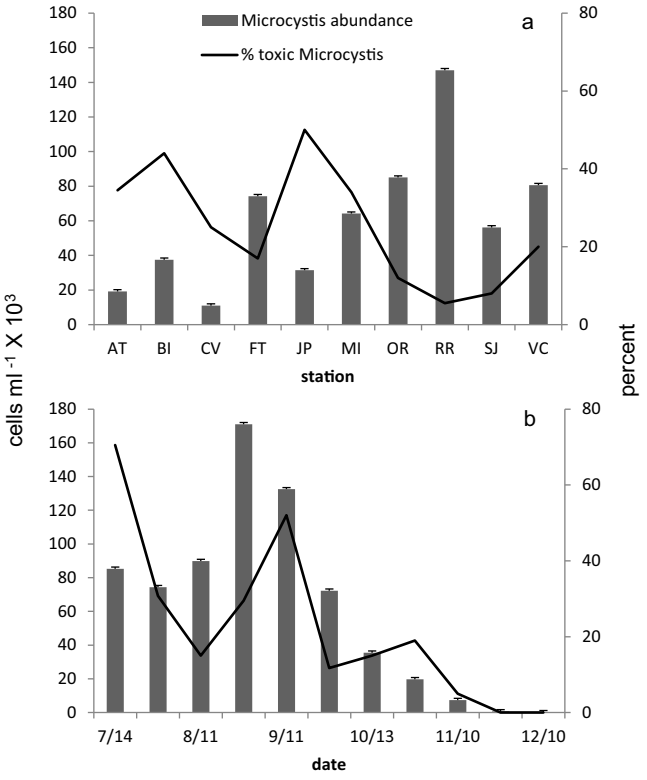

Fig. 8. *Microcystis* abundance (line) and the percentage of potentially toxic *Microcystis* cells containing the *mcyD* gene for toxin production (bar) measured by qPCR for all size fractions in whole water samples from 0.3 m depth by station (a) and month (b) between July and December 2014.

On average, potentially toxic *Microcystis* cells comprised 21 ± 24% of the *Microcystis* cells in the bloom. The number of potentially toxic *Microcystis* cells increased with *Microcystis* abundance ($r = 0.87$, $p < 0.01$), but the percent of toxic *Microcystis* cells was variable and poorly correlated with *Microcystis* abundance ($r = 0.31$, $p < 0.01$; Fig. 8). The percentage of potentially toxic cells varied little among stations, and was only greater ($p < 0.05$) at station JP than stations SJ and RR (Fig. 8a). Among months, the percent of potentially toxic *Microcystis* cells was greater ($p < 0.05$) in summer than fall (Fig. 8b).

3.5. Correlation among variables

Microcystis abundance ($r = 0.82$), as well as the number of toxic *Microcystis* cells ($r = 0.77$; $p < 0.01$) measured by qPCR were correlated with the chlorophyll *a* concentration in the surface net tow (Table 3). The chlorophyll *a* concentration in the surface net tow, and both *Microcystis* and toxic *Microcystis* abundance increased with water temperature, pH, percent dissolved oxygen, and total phosphorus, and were associated with reduced concentrations of both nitrate and ammonium (Table 4). *Microcystis* abundance varied directly with *Dolichospermum* ($r = 0.53$) and *Aphanizomenon* ($r = 0.73$) abundance, as well as total cyanobacteria abundance ($r = 0.91$, $p < 0.01$). *Dolichospermum*, *Aphanizomenon* and total cyanobacteria abundance also increased with water temperature and pH, but unlike *Microcystis*, *Dolichospermum* and *Aphanizomenon* also increased with total and dissolved organic carbon. *Dolichospermum* and *Aphanizomenon* were negatively correlated with specific conductance, total suspended solids and total dissolved solids, while *Microcystis* was not. *Aphanizomenon* was also negatively correlated with turbidity, while *Dolichospermum* was not.

3.6. Historical comparisons

The difference between both chlorophyll *a* and total microcystin concentration measured in 2014 and previous wet years increased the historical difference in biomass and toxin concentration measured between wet and dry year types by over an order of magnitude. The median chlorophyll *a* concentration in surface net tows during August and September of 2014 was 9 to 12 times greater ($p < 0.05$) than in previous dry or wet years, respectively (Table 5). Similarly, total microcystin concentration in the water column increased ($p < 0.05$) by 11 to 65 times in 2014 compared with previous dry or wet years, respectively.

Environmental variables differed among water year types during the peak of the *Microcystis* bloom in August and September, but few variables demonstrated a linear increase with dry conditions. Specific conductance was greater in both 2014 and dry years than wet years, by at least a factor of two (Table 5). The pH also increased with dry conditions, but was greater in dry years than 2014. Water temperature did not differ among year types, but dissolved oxygen concentration was greater in wet and dry years than 2014. Water transparency also did not differ among year types based on turbidity, total suspended solids concentration and areal light levels in the euphotic zone.

For nutrients, there was no difference in nitrate or silicate concentration among water year types in August and September, but ammonium concentration was lower ($p < 0.05$) in 2014 than previous wet or dry year types (Table 5). Even though ammonium concentration was relatively low in 2014, it was the primary nitrogen source for the bloom. The δ^{15}N-nitrate to δ^{15}N-POM

Table 3
Spearman correlation coefficients computed between *Microcystis*, *Dolichospermum*, *Aphanizomenon* and total cyanobacteria abundance in whole water samples measured by qPCR and chlorophyll *a* and phaeophytin concentration in surface net tow samples collected twice each month between July and December 2014 at 10 stations. Correlations were either significant at the 0.01 level or not significant (blank).

	chlorophyll *a*	phaeophytin	*Microcystis*	toxic *Microcystis*	*Dolichospermum*	*Aphanizomenon*
phaeophytin	0.62					
Microcystis	0.82	0.52				
toxic *Microcystis*	0.77	0.50	0.87			
Dolichospermum	0.42	ns	0.53	0.54		
Aphanizomenon	0.51	0.31	0.73	0.52	0.52	
total cyanobacteria	0.77	0.45	0.91	0.58	0.58	0.72

Table 4
Spearman rank correlation coefficients computed between environmental variables, chlorophyll *a* concentration in surface net tows and the abundance of cyanobacteria determined by qPCR measured twice each month, between July and December 2014, at 10 stations in the San Francisco Estuary. Significance is indicated at the 0.05 level (regular type), 0.01 (bold type) or not significant (blank).

	chlorophyll *a*	*Microcystis*	toxic *Microcystis*	*Dolichospermum*	*Aphanizomenon*	total cyanobacteria
water temperature, °C	**0.77**	**0.82**	**0.78**	**0.55**	**0.57**	**0.88**
specific conductance, µS cm^{-1}				**−0.35**	**−0.39**	**−0.29**
chloride, mg l^{-1}				**−0.34**	**−0.40**	**−0.30**
turbidity, NTU					**−0.28**	
total dissolved solids, mg l^{-1}				**−0.33**	**−0.37**	**−0.28**
total suspended solids, mg l^{-1}				−0.24	**−0.33**	
dissolved oxygen, mg l^{-1}						−0.22
pH	**0.62**	**0.60**	**0.59**	**0.31**	**0.40**	**0.59**
ammonium, mg l^{-1}	**−0.52**	**−0.58**	**−0.57**	**−0.49**	**−0.46**	**−0.61**
nitrate, mg l^{-1}	**−0.44**	**−0.54**	**−0.54**	**−0.44**	**−0.47**	
solube reactive phosphorus, mg l^{-1}						
total phosphorus, mg l^{-1}	**0.43**	**0.42**	**0.36**			**0.49**
N:P molar ratio	**−0.60**	**−0.71**	**−0.63**	**−0.50**	**−0.63**	**−0.77**
silica, mg l^{-1}	**−0.59**	**−0.54**	**−0.63**	**−0.46**	**−0.36**	**−0.70**
dissolved organic nitrogen, mg l^{-1}	**0.29**					**0.27**
total organic carbon, mg l^{-1}		0.24		0.21	**0.36**	**0.35**
dissolved organic carbon, mg l^{-1}		0.19			**0.33**	**0.29**
volatile suspended solids, mg l^{-1}					−0.20	

isotope ratio was less than 1 for all but 14 samples taken during the 2014 bloom season (Fig. 9). Such low isotope ratios indicated that there was little use of nitrate as a nitrogen source across the Delta. Among stations, nitrate was most often used as a nitrogen source by primary producers (δ^{15}N-nitrate to δ^{15}N-POM isotope ratio > 1) at station RR (not shown).

SRP increased with dry conditions, but was anomalously high in 2014, when it reached the highest concentration measured in 22

Table 5
Comparison of median physical, chemical and biological variables measured during the peak of the *Microcystis* bloom in August and September at stations AT, CV, SJ and OR for wet years 2004 and 2005 (W), dry years 2007 and 2008 (D) and the critically dry year 2014 (C). *Microcystis* abundance was determined by microscopy. Relative differences between water years were significantly different at the 0.05 level or higher.

variable	wet	dry	2014 critical	significant difference
Microcystis in net tow, log cells ml^{-1}	1.24 ± 1.84	4.4 ± 0.12	5.07 ± 1.09	C > D, W; D > W
total microcystins, µg l-1	0.01 + 0.01	0.06 + 0.08	0.65 ± 0.23	C > D, W; D > W
chlorophyll *a in net tow,* µg l^{-1}	0.08 ± 0.09	0.11 ± 0.12	0.98 ± 0.83	C > D, W; D > W
phaeophytin in net tow, µg l^{-1}	6.8E−3 ± 7.1E-3	0.04E−3 ± 0.06E-3	0.05 ± 0.04	C > D, W
water temperature, °C	22.7 ± 2	21.8 ± 2	22 ± 2	ns
euphotic zone light µmol photons m^{-1} s^{-1}	912 ± 347	1154 ± 589	893 ± 231	ns
specific conductance, µS cm^{-1}	361 ± 246	752 ± 772	2461 ± 3092	D,C > W
chloride, mg l^{-1}	96 ± 119	167 ± 203	673 ± 909	C > W
total suspended solids, mg l^{-1}	6 ± 5	6 ± 5	10 ± 11	ns
volatile suspended solids, mg l^{-1}	2 ± 1.5	1 ± 1.5	2.0 ± 1.5	C,W > D
dissolved oxygen, mg l^{-1}	8.8 ± 0.8	8.6 ± 0.5	8.0 ± 0.3	W, D > C
pH	7.9 ± 0.3	8.2 ± 0.4	8.0 ± 0.2	D,C > W; D > C
turbidity	8.4 ± 8.4	5.9 ± 4.5	8.6 ± 6.7	ns
ammonium, mg l^{-1}	0.03 ± 0 0.01	0.03 ± 0.01	0.02 ± 0.01	D > C
nitrate, mg l^{-1}	0.23 ± 0.07	0.28 ± 0.09	0.21 ± 0.15	ns
Soluble reactive phosphorus, mg l^{-1}	0.05 ± 0.01	0.06 ± 0.01	0.09 ± 0.02	C > W,D; D > W
NP ratio	11.4 ± 4.4	11.9 ± 3.3	7.1 ± 3.8	D,W > C
silica, mg l^{-1}	14.1 ± 1	14.6 ± 1	13.7 ± 1	ns
total organic carbon, mg l^{-1}	2.2 ± 0.5	2.2 ± 0.3	2.8 ± 0.6	C > W,D
dissolved organic carbon, mg l^{-1}	1.9 ± 0.30	2.1 ± 0.2	3.0 ± 0.5	C > W,D; D > W
Sacramento River-Freeport, m^3 s^{-1}	495 ± 31	334 ± 84	239 ± 19	W > D, C; D > C
Sacramento River-Rio Vista, m^3 s^{-1}	272 ± 28	160 ± 66	95 ± 11	W > D, C; D > C
San Joaquin River-Vernalis, m^3 s^{-1}	47 ± 25	27 ± 3	9 ± 1	W > D, C; D > C
San Joaquin River-Jersey Point, m^3 s^{-1}	−95 ± 23	−70 ± 64	3 ± 16	C > D, W; D > W
SWP agricultural diversion m^3 s^{-1}	203 ± 1	92 ± 95	48 ± 21	W > D, C; D > C
CVP agricultural diversion m^3 s^{-1}	125 ± 1	123 ± 3	23 ± 24	W > D, C; D > C

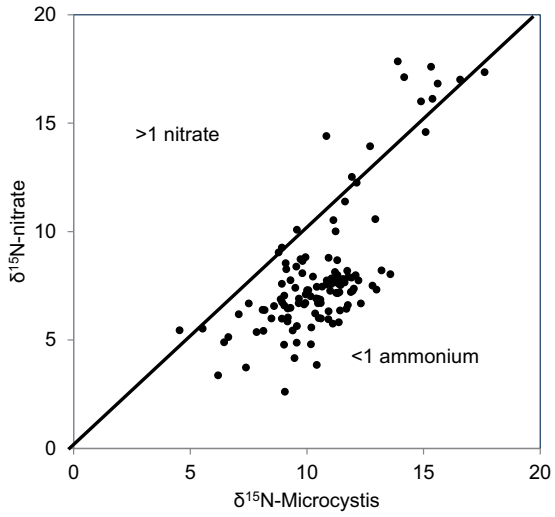

Fig. 9. Ratio of the δ^{15}N-nitrate in the water column and the δ^{15}N-particulate organic matter in *Microcystis* surface net tows measured between July and December 2014 at all stations. n = 109.

years (0.09 ± 0.01 mg l^{-1}; Fig. 10). The elevated SRP concentration in 2014 caused the N:P molar ratio to decrease to the lowest value (7.1) measured in two decades at station OR. Median SRP concentration at station OR was 0.08 ± 0.03 mg l^{-1} between 1975 and 1992, declined to 0.05 ± 0.01 mg l^{-1} between 1993 and 2013 and then increased to 0.09 ± 0.01 mg l^{-1} in 2014. Similar changes in SRP concentration were measured for the long-term monitoring station at CV (not shown).

Total and dissolved organic carbon concentration increased with dry conditions and was greater in 2014 than dry years ($p < 0.05$; Table 5). Some of the increase in total organic carbon in 2014 was due to the increase in chlorophyll *a* concentration. However, some of the increase in total and dissolved organic carbon in 2014 was probably associated with other organic matter, because total volatile suspended solids concentration was twice as high in 2014 than dry years.

Water temperatures in 2014 reached some of the highest values measured in the previous 10 years (Fig. 11). Median water temperature, computed from continuous water temperature measurement s at Stockton on the San Joaquin River, was higher at the beginning of the bloom in May 2014 ($p < 0.05$) than in May 2005, 2006, 2010, 2011 or 2012. By June, water temperature reached a 10 year high ($p < 0.05$; median 24.5 °C). *Microcystis* biovolume peaked in July 2014, when the median water temperature was 26.0 °C, which was a highest water temperature measured in 5 of the previous 10 years (2005, 2007, 2010, 2011 and 2012). Warmer median water temperature also occurred in August, September and November 2014 than 9 of the previous 10 years, while October (22.1 °C) and December (12.6 °C) had the highest ($p < 0.05$) median water temperature measured since 2004. In addition, while median water temperature remained above 18 °C between May and October, minimum water temperature remained above 15 °C through November. The decline of the bloom in December was characterized by the decrease of water temperature below 15 °C.

The 2014 drought year was characterized by a large reduction in both inflow and water removal by agricultural diversion compared with previous years. At the peak of the bloom in August and September, median Sacramento River streamflow into the Delta at Freeport and within the Delta at Rio Vista was lower by 52% and 65% than previous wet years and by 28% and 41% than previous dry years, respectively (Table 5). The largest decrease in streamflow into the Delta occurred at Vernalis on the San Joaquin River, where streamflow decreased by 81% and 67% in 2014 compared with previous wet and dry years, respectively. The 2014 drought was also characterized by large reductions in agricultural diversion. Agricultural diversion at both CVP and SWP facilities were 82% and 76% less in 2014 compared with wet years, and exceeded reductions in previous dry years by 81% and 48%, respectively. The reduced removal by agricultural diversion was further demonstrated by the downstream (positive) streamflow at Jersey Point in 2014, compared with the upstream (negative) streamflow in wet years, when removal of water for agriculture reverses streamflow (Table 5). Together low streamflow and agricultural diversion created a monthly median streamflow in the San Joaquin River at Vernalis of only 8.6 m^3 s^{-1} (range 7.9–9.2 m^3 s^{-1}) between June and September 2014.

4. Discussion

4.1. Bloom amplitude

Microcystis biomass in 2014 reached record levels and greatly expanded the range of bloom conditions in SFE. The difference between median chlorophyll *a* concentration in 2014 and previous

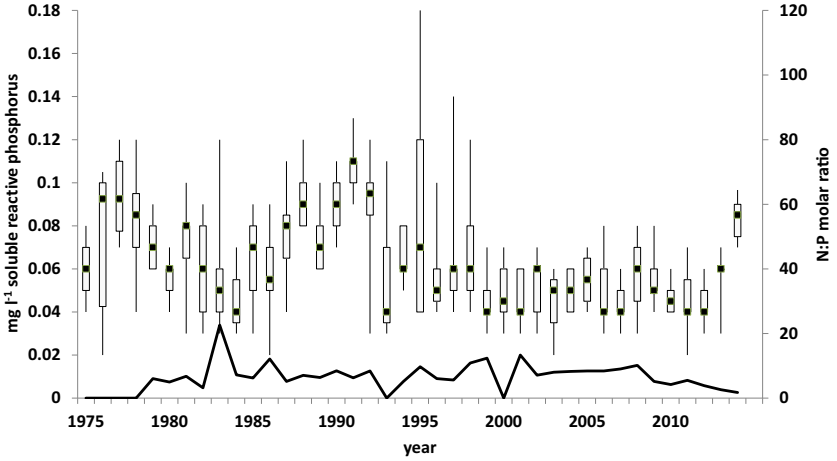

Fig. 10. Median and standard deviation of soluble reactive phosphorus concentration and the N:P molar ratio measured during August and September between 1975 and 2014 at station OR.

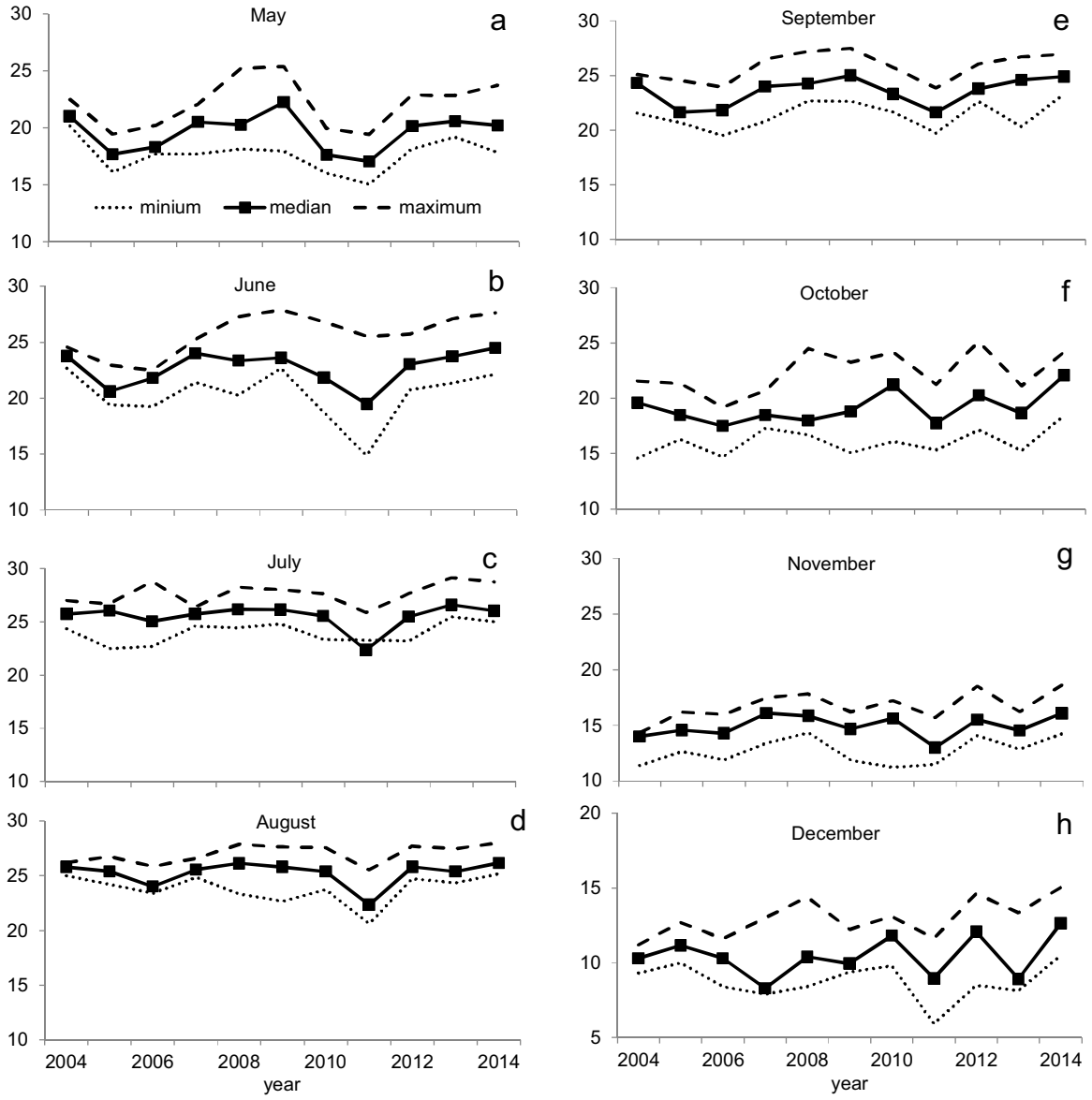

Fig. 11. Maximum (dashed line), median (solid line) and minimum (dotted line) monthly water temperature computed from continuous data collected between May and December (a-h) for 1975 through 2014 at Old River station OR. Note the axis change for December.

wet years was over an order of magnitude greater than between previous wet and dry years. Chlorophyll *a* concentration associated with cyanobacteria biomass also increased at low streamflow in the Neuse River Estuary (Paerl et al., 2006), but the relative increase compared with wet conditions was greater for SFE in 2014. Although the maximum chlorophyll *a* concentration (31 μg l^{-1}) in the surface net tows during the 2014 *Microcystis* bloom was the highest measured for SFE, the biomass was relatively low compared with many *Microcystis* blooms worldwide. Chlorophyll *a* concentration associated with *Microcystis* blooms reached 1000 μg l^{-1} in Lake Taihu, China, 479 μg l^{-1} in the Nakong River, South Korea, 160 μg l^{-1} in Caldeiras and Mondego River, Portugal, 10 μg l^{-1} in the Neuse River and 20 μg l^{-1} in the Chesapeake River Estuaries, USA and 602 μg l^{-1} in nearby Klamath River, USA (Ha et al., 1999; Moisander et al., 2009; de Figueiredo et al., 2012; Otten et al., 2012).

The relatively low chlorophyll *a* concentration in SFE during the bloom was partly due to the net sample, which was an integrated sample of only the wide diameter colonies in the upper 0.3 m of the water column, and not a sample of the concentrated surface scum. However, relatively low chlorophyll *a* concentration is common in SFE, where light limitation due to high levels of suspended solids and a deep water column (13 m) leads to a net negative carbon production of the water column (Jassby, 2008; Lehman et al., 2013). Some *Microcystis* may be lost to grazing by clams, especially during vertical migration. Clam grazing can significantly depress phytoplankton biomass in the Delta, particularly in the shallow marine bays (Kimmerer, 2004). However, clam grazing has little impact on *Microcystis* colonies in the surface layer of the main river channels that are often 13 m deep (Dugdale et al., 2016).

The total microcystin concentration in 2014 was also the highest on record in SFE, and made the water toxic for both humans and wildlife. Like chlorophyll *a* concentration, the difference between the total microcystin concentration in 2014 and wet years was over an order of magnitude greater than measured previously between wet and dry years, and greatly expanded the range of conditions measured in the estuary. Total microcystin concentration frequently exceeded guidelines for microcystin in drinking

water suggested by the World Health Organization of 1 $\mu g\,l^{-1}$ for adults, and continually exceeded guidelines established by the U. S. Environmental Protection Agency of 0.3 $\mu g\,l^{-1}$ for children under the age of 6 (World Health Organization, 2011; United States Environmental Protection Agency, 2015). The positive correlation between the abundance of toxic *Microcystis* cells and total *Microcystis* abundance indicated the large bloom in 2014 was associated with more toxins in the water column, but the association was highly variable. The percent of toxic *Microcystis* cells only reached about 20% in 2014, and like previous dry years, varied by a factor of 10 among stations (Baxa et al., 2010). Microcystin concentration generally increases with *Microcystis* biomass, but the correlation is usually not linear, because the cellular content of microcystins can vary by a factor of 50 (Zurawell et al., 2005).

The factors that controlled microcystin production in 2014 were not clear. Batch culture experiments suggested that microcystins increase in response to high light and oxidative stress (Zilliges et al., 2011). In addition, a poor correlation between chlorophyll *a* and total microcystin concentration during the peak of the bloom was thought to be due to reduced toxin production at low light conditions caused by self-shading (Van de Waal et al., 2009). In SFE, there was no significant difference in light levels within the euphotic zone during the peak of the bloom and the lack of a surface scum in SFE probably limited the influence of self-shading. Instead, the low total microcystin concentration during the peak of the bloom in 2014 may have been due to a change in the *Microcystis* strain or genotype. The presence of different *Microcystis* strains was suggested by the presence of 11 microcystin congeners in SFE (Lehman et al., 2008). Genotype succession accounted for shifts from toxic to non-toxic blooms in lake environments in the Netherlands (Kardinaal et al., 2007). A shift from toxic to non-toxic *Microcystis* bloom strains was also associated with a change in light availability in Lake Taihu, China (Otten et al., 2012). It is possible that there were other cyanobacteria present that affected the microcystin concentration in SFE. Total cyanobacteria were more abundant than *Microcystis* and many other genera can produce microcystins.

4.2. Bloom timing

Elevated water temperature contributed to the extended *Microcystis* bloom season in 2014 that spanned 8 months, and was twice as long as previous bloom seasons (Lehman et al., 2013). It is anticipated that increased water temperature associated with climate change will extend the duration of cyanobacteria blooms (Paerl and Huisman, 2009). In California, climate change models and in situ measurements predicted a long-term increase in winter and early spring air temperature that could extend the duration of the *Microcystis* bloom by allowing it to start earlier in the spring (Cayan et al., 2009). Elevated water temperature in the spring of 2014 extended the bloom by at least two months. However, the duration of the *Microcystis* bloom in 2014 bloom was also extended another two months by elevated warm water temperature in the fall and early winter. Elevated spring water temperature may also affect the duration of the peak of the bloom. The peak of the *Microcystis* bloom began in July for 2014, a month earlier than for previous blooms, and suggested future blooms may not only last longer, but have a longer period of peak biomass with elevated water temperature in the spring (Lehman et al., 2013).

4.3. Genetic diversity

Cyanobacteria were more abundant and diverse in 2014 than in previous years. Cyanobacteria comprised 50% to 80% of the primary producer community in 2014, with relatively little of the total cyanobacteria abundance associated with *Microcystis* (19%). In contrast, *Microcystis* comprised over 90% of the of the primary producer biomass in the dry years 2007 and 2008 (Lehman et al., 2010). *Microcystis* spp. also co-varied with *Aphanizomenon* spp. and *Dolichospermum* spp. throughout much of the bloom for the first time in 2014. *Microcystis, Aphanizomenon and Dolichospermum* are characterized by a succession from *Dolichospermum* and *Aphanizomenon* to *Microcystis* spp. as water temperature increases in lakes and rivers worldwide, including Aguieira Reservoir and Guadiana River, Portugal (Vasconcelos et al., 2011; de Figueiredo et al., 2012), Lake Yogo, Japan (Tsukada et al., 2006) and Lake Karaoun, Lebanon (Atoui et al., 2013). The co-occurrence of these genera in SFE may signal a successional shift to a more complex cyanobacterial community composition than occurred during the initial *Microcystis* bloom, which only began in 1999 (Lehman et al., 2005).

Some cyanobacteria are thought to promote the abundance and diversity of cyanobacteria by releasing allelopathic chemicals or nutrients (Sedmak and Eleršek, 2006; Suikkanen et al., 2005). The frequent presence of *Aphanizomenon* and *Dolichospermum* and abundance of other cyanobacteria in SFE throughout the 2014 bloom may have been due to the preconditioning of the water by *Microcystis* for other cyanobacteria. As nitrogen fixers, *Aphanizomenon* and *Dolichospermum* often fix nitrogen that can promote the growth of *Microcystis*, a non-nitrogen fixing species (Ferber et al., 2004). However, nitrogen fixation by other cyanobacteria was probably not a primary driver of *Microcystis* growth in 2014, because total nitrogen concentration was usually in excess, and vertical migration of *Microcystis* to the bottom of the water column could provide access to additional ammonium released near the sediment surface or recycled within the water column (Imai et al., 2009; Cornwell et al., 2014).

Instead, it is likely that *Aphanizomenon* and *Dolichospermum* were co-occurring species that used slightly different habitats than *Microcystis*. The use of different habitats by *Aphanizomenon* and *Dolichospermum* was supported by the stronger correlation of these two species with low specific conductance and turbidity, and total and dissolved organic carbon than *Microcystis* in 2014. *Aphanizomenon* and *Anabaena* also occur at lower water temperature and require more light to grow than *Microcystis* (Fadel et al., 2015; Ferber et al., 2004; Wu et al., 2016), which may explain their greater abundance at the beginning and end of the 2014 bloom season. The influence of low water temperature on *Aphanizomenon* abundance in SFE was further demonstrated in the summer of 2011, when *Aphanizomenon* dominated the primary producer community due to unseasonably cool water temperature and high streamflow (Kurobe et al., 2013).

The 2014 bloom was also characterized by an increase in the number of *Microcystis* species. The first *Microcystis* species identified in the Delta was *Microcystis aeruginosa* (Lehman et al., 2005), and it remained the only *Microcystis* species identified by microscopy through 2008 (Lehman et al., 2013). Different microcystin congeners suggested there were multiple strains of *Microcystis* within the bloom, and initial genetic analysis suggested there were potentially different *Microcystis* genotypes in the central and western Delta (Lehman et al., 2008, 2013; Moisander et al., 2009). However, during the 2014 drought, three *Microcystis species morphotypes* were visible for the first time, *M. aeruginosa*, *M. wesenbergii* and *M. flos-aquae*. It is common for more than one *Microcystis* species to occur during blooms, so the additional species in 2014 may indicate a natural bloom succession. It is unknown if the *Microcystis* species identified microscopically in SFE are genetically unique. Of four visually different *Microcystis* species identified in Lake Taihu, China, M. *aeruginosa*, M. *flos-aquae*, M. *ichtohyblake* and M. *wesenbergii,* only M. *wesenbergii* was genetically unique (Otten and Paerl, 2011).

4.4. Environmental factors

Elevated water temperature appeared to be a key factor controlling the magnitude and duration of the *Microcystis* bloom in 2014. Water temperature was strongly correlated with chlorophyll *a* concentration, toxic *Microcystis* cell abundance and total microcystin concentration in 2014. Water temperature was similarly correlated with *Microcystis* biomass in previous years for SFE (Lehman et al., 2008). Water temperature of 19 °C is needed to initiate growth of *Microcystis* blooms in the Delta (Lehman et al., 2013), and is a common threshold for initiation of *Microcystis* growth in the spring worldwide (Latour et al., 2004; Jiang et al., 2008). Maximum water temperature of 23.7 °C and median water temperature of 20.2 °C in May 2014 probably contributed to the early start of the *Microcystis* bloom, which was two months earlier than usual for SFE. During the summer, median water temperatures at or above 25 °C between June and September were ideal for cyanobacteria growth. Cyanobacteria, particularly *Microcystis*, increase at water temperatures at or above 25 °C, where they can out-compete other primary producers (Paerl and Paul, 2012). *Microcystis* blooms can also persist in the surface layer, as long as water temperature remains above 15 °C, even if light levels are below those needed for growth (Robarts and Zohary, 1987). Record median water temperature for October through November at above 15 °C and maximum water temperature of 15 °C in December enabled the 2014 *Microcystis* bloom to extend into the winter. Elevated water temperature near the surface can also cause stratification of the water column, which enhances *Microcystis* biomass by keeping *Microcystis* colonies in the surface layer, where light is available for photosynthesis (Paerl and Paul, 2012). However, stratification is probably less important in SFE, where a combination of tide, current and wind mix the water column daily.

The elevated water temperature in 2014 may also have contributed to the relatively high levels of total microcystin in the *Microcystis* bloom. *Microcystis* biomass and total microcystin concentration co-occurred with the peak water temperatures in July. Total microcystin concentration also increased with water temperature in Daechung Reservoir, Korea and Steilacoom Lake, Washington (Joung et al., 2011; Jacoby et al., 2000). Genetic analysis suggested that the number of genes or transcripts associated with microcystin production increase with water temperature (Davis et al., 2009; Kim et al., 2005). However, it is still unclear why microcystins are produced in *Microcystis* cells or why they increase with water temperature (Paerl and Otten, 2013).

High residence time was another key environmental factor that contributed to the magnitude of the 2014 *Microcystis* bloom in SFE. A combination of decreased inflow from the major rivers and removal by agricultural diversion increased the residence time and resulted in accumulation of *Microcystis* colonies in the Delta. Accumulation is an important mechanism controlling the magnitude of *Microcystis* blooms, because *Microcystis* has a slow growth rate (Reynolds, 1997). The maximum biomass-specific growth rate measured during the 2004 *Microcystis* bloom was only 0.36–1.15 mg C (mg chlorophyll a)$^{-1}$ h^{-1} (Lehman et al., 2008), and was three times lower than the maximum biomass-specific growth rate of non-*Microcystis* primary producers measured in the Yolo Bypass and Sacramento River (Lehman, 2004). Flushing time was also a key factor controlling the magnitude of cyanobacteria blooms in Lower Darling River, Australia, where streamflows of 3.5 m^3 s^{-1} and 34.7 m^3 s^{-1} prevented stratification and cyanobacteria bloom formation, respectively (Mitrovic et al., 2011). Modeling studies in the Dutch Delta, the Netherlands also suggested that *Microcystis* blooms with a chlorophyll *a* concentration greater than10 μg l^{-1} only occurred when streamflow was less than 65 m^3 s^{-1} (Verspagen et al., 2006). By comparison, relatively small *Microcystis* blooms occurred in the 2004 and 2005 wet years, when San Joaquin River streamflow was between 28.32–35.40 m^3 s^{-1} (Lehman et al., 2008). A factor of three lower San Joaquin River streamflow (9.1 m^3 s^{-1}) was needed to produce the large 2014 *Microcystis* bloom.

The role of streamflow in *Microcystis* bloom development within SFE differed from other estuaries, where nutrient concentrations are low. In nutrient poor estuaries, high streamflow is needed prior to the bloom in order to flush nutrients needed for growth into the estuary. In the Swan River Estuary, Australia, the Hartbeaspoort dam reservoir, South Africa and the Potomac and Neuse River Estuaries, USA, *Microcystis* blooms in drought years were preceded by high precipitation events that flushed nutrients needed to support the cyanobacteria bloom into the region (Paerl and Otten, 2013). High streamflow in these estuaries also cause stratification, which kept *Microcystis* colonies on the surface of the water column, where light was available. In contrast, excess nutrient concentration characterizes SFE year round from a combination of discharge from point and non-point sources, as well as low uptake from primary producers due to light limitation (Jassby, 2008), and stratification is limited by tide.

Although nitrate concentration was always above detection limits and dominated the dissolved inorganic nitrogen pool, ammonium was the primary source of nitrogen for the *Microcystis* bloom during 2014. Ammonium was also the primary source of nitrogen during the *Microcystis* blooms in the dry years 2007 and 2008 (Lehman et al., 2015). However, it was surprising that ammonium remained the primary source of nitrogen for the bloom in 2014, because the ammonium concentration was low and sometimes below the reporting limit of 0.01 mg l^{-1}, while nitrate concentration remained relatively high. A high ammonium uptake rate combined with a low growth rate may enable *Microcystis* to grow or survive on low ammonium concentration (Jacoby et al., 2000; Lehman et al., 2008; Lee et al., 2015). It is also possible that access to small amounts of ammonium from rapid mineralization processes within the water column or sediment flux near the bottom during daily vertical migration is sufficient for *Microcystis* to survive.

There was no clear link between the anomalous increases in SRP in 2014 and elevated *Microcystis* biomass or chlorophyll *a* concentration. Bioassays suggested the addition of only soluble reactive phosphorus does not enhance growth in *Microcystis* blooms, in Klamath River, Oregon, Lake Taihu, China or Lake Erie, Michigan (Moisander et al., 2009; Xu et al., 2010; Chaffin et al., 2013). It is also unknown if the low N:P molar ratio produced by the elevated SRP concentration had a major influence on *Microcystis* growth in SFE. Total nitrogen and SRP concentrations were well in excess during the *Microcystis* bloom and the N:P ratio was not correlated with *Microcystis* biovolume (Lehman et al., 2008,2013). SRP concentration could have enhanced microcystin production. Increased SRP was associated with high cellular microcystin content in *Anabaena* spp. (Rapala et al., 1997). A low N:P molar ratio was also associated with enhanced production of toxin producing *Microcystis* in Lake Taihu, China (Otten et al., 2012).

The role of light on the magnitude and toxin concentration of the *Microcystis* bloom in 2014 is unclear. SFE is one the most turbid estuaries in the world due to high levels of sediment, which causes light limitation of primary productivity (Jassby, 2008). Vertical migration to the surface would enable *Microcystis* to avoid light limitation within the water column. However, the strong positive correlation between *Microcystis* abundance and light levels in the water column suggests *Microcystis* grows better in SFE when there is more light in the water column (Lehman et al., 2008,2013). Elevated euphotic zone light levels may have contributed to the relatively high *Microcystis* abundance in the San Joaquin River, where the light levels were greater than those in the Sacramento

River. Although light levels in the euphotic zone were not greater in 2014 than previous years during the peak of the bloom, the persistence of elevated euphotic zone light levels during mid-day throughout the fall may have contributed to the long duration of the bloom. It is also possible that *Microcystis* was able to survive at sub-optimal light conditions at the end of the season, even if it wasn't able to grow. *Microcystis* was able to survive, but not grow, at a combination of low light and low water temperature in Hartbeespoort Dam, South Africa (Robarts and Zohary, 1987).

Light levels may have influenced microcystin production in 2014. Recent research suggested microcystin production may be a defense mechanism against the ultraviolet light in sunlight (Zilliges et al., 2011). In Lake Taihu, China, the presence of more genes associated with toxin production at high light intensities was hypothesized to be needed for the protection of colonies from photoinhibition (Otten et al., 2012). A defense mechanism against high light intensity might be needed in the Mediterranean climate of SFE, where *Microcystis* colonies are concentrated within the first 0.3 m of the water column and surface irradiance levels reach near 2000 μmol photons m^{-2} s^{-1} throughout the summer at mid-day. Elevated dissolved total microcystin concentration and total microcystin concentration in July and/or August, suggested microcystins could have served as a protection against high surface irradiance in the summer of 2014.

4.5. Drought impacts

Based on the 2014 severe drought, future increases in the frequency and intensity of drought in California will likely lead to an increase in the frequency and intensity of cyanobacteria blooms in SFE (Cayan et al., 2009; Lehman et al., 2013). Warmer water temperature throughout the year will cause *Microcystis* blooms to occur earlier in the spring and extend longer into the fall and winter, perhaps becoming a continuous year-long bloom (Paerl and Paul, 2012). The combination of both increased frequency of elevated water temperature and low flushing rate will increase the intensity of *Microcystis* and other cyanobacteria blooms through both enhanced growth and accumulation, respectively. In addition, the presence of *Microcystis* and other cyanobacteria may create water quality conditions that favor the growth of cyanobacteria over other primary producers that are more favorable for the aquatic food web (Lehman et al., 2010). Lastly, the presence of all cyanobacteria will increase the potential development of elevated toxin concentrations that can adversely impact the health and survival of aquatic foodweb species, including phytoplankton, zooplankton and fish (Lehman et al., 2008; Ger et al., 2009, 2010; Acuña et al., 2012a, 2012b).

5. Conclusion

The *Microcystis* bloom during the 2014 severe drought had the highest biovolume, toxin concentration, cyanobacteria diversity and the longest duration compared with previous blooms in SFE and expanded the range of conditions in the estuary. The difference in chlorophyll *a* and total microcystin concentration between wet and dry years increased by at least an order of magnitude with the 2014 drought. Elevated water temperature was a key factor controlling the severity of the bloom and was correlated with both *Microcystis* and toxic *Microcystis* abundance. Elevated water temperature in both the spring and fall also contributed to an increase in the duration of the bloom from four to eight months. Low streamflow combined with low agricultural diversion contributed to the magnitude of the bloom by enabling *Microcystis* biomass to accumulate. The 2014 severe drought study suggested anticipated future increases in the frequency and intensity of drought in SFE will lead to an increase in the magnitude, duration, diversity and toxic potential of *Microcystis* blooms in SFE.

Acknowledgements

Funding for this project was obtained from the California Department of Water Resources and Department of Fish and Wildlife Drought Response Program. Field assistance was provided by M. Dempsey, E. Santos, N. van Ark, S. Waller, T. Hollingshead, R. Elkins, H. Fuller, M. Legro, A. Lopez, M. Martinez, A. Munguia, M. Ogaz and L. Smith. Laboratory assistance was provided by the DWR Bryte Laboratory, M. Xiong, E. Jeu, R. Mulligan and A. Lopez. Administrative assistance was provided by K. Gehrts and S. Phillipart.[CG]

References

Acuña, S.C., Baxa, D., Teh, S.J., 2012a. Sublethal dietary effects of microcystin producing *Microcystis* on threadfin shad, *Dorosoma petenense*. Toxicon 60, 1191–1202.

Acuña, S.C., Deng, D.-F., Lehman, P.W., Teh, S.J., 2012b. Dietary effects of *Microcystis* on Sacramento splittail, *Pogonichthys macrolepidotus*. Aquat. Toxicol. 110-111, 1–8.

American Public Health Association, American Water Works Association, Water Environment Association, 1998. Standard Methods for the Examination of Water and Wastewater. 20th Edition. American Public Health Association, Washington, D.C., USA.

Atoui, A., Hafez, H., Slim, K., 2013. Occurrence of toxic cyanobacterial blooms for the first time in Lake Karaoun, Lebanon. Water Environ. J. 27, 42–49.

Baxa, D.V., Kurobe, T., Ger, K.A., Lehman, P.W., Teh, S.J., 2010. Estimating the abundance of toxic *Microcystis* in the San Francisco Estuary using quantitative Q-PCR. Harmful Algal Blooms 9, 342–349.

Cayan, D., Tyree, M., Dettinger, M., Hidalgo, H., Das, T., Maurer, E., Bromirski, P., Graham, N., Flick, R., 2009. Climate Change Scenarios and Sea Level Rise Estimates for the California 2009 Climate Change Scenarios Assessment. California Climate Change Center CEC-500-2009-014-D.

Chaffin, J.D., Bridgeman, T.B., Bade, D.L., 2013. Nitrogen constrains the growth of late summer cyanobacterial blooms in Lake Erie. Adv. Microbiol. 3, 16–26.

Codd, G.A., 2000. Cyanobacterial toxins, the perception of water quality, and the prioritization of eutrophication control. Ecol. Eng. 16, 51–60.

Cornwell, J.C., Glibert, P.M., Owens, M.S., 2014. Nutrient fluxes from sediments in the San Francisco Bay Delta. Estuar. Coasts 37, 1120–1133.

Davis, T.W., Berry, D.L., Boyer, G.L., Gobler, C.J., 2009. The effects of temperature and nutrients on the growth and dynamics of toxic and non-toxic strains of *Microcystis* during cyanobacteria blooms. Harmful Algae 8, 715–725.

e Figueiredo, D.R., Castro, B.B., Pereira, M.J., Correia, A., 2012. Bacterioplankton community composition in Portuguese water bodies under a severe summer drought. Commun. Ecol. 13, 185–193.

Dugdale, R.C., Wilkerson, F.P., Parker, A.E., 2016. The effect of clam grazing on phytoplankton spring blooms in the low salinity zone of the San Francisco Estuary: a modeling approach. Ecol. Model. 340, 1–16.

Elliott, J.A., 2012. Is the future blue-green? A review of the current model predictions of how climate change could affect pelagic freshwater cyanobacteria. Water Res. 46, 1364–1371.

Fadel, A., Atoui, A., Lemaire, B.J., Vincon-Leite, B., Slim, K., 2015. Environmental factors associated with phytoplankton succession in a Mediterranean reservoir with a highly fluctuating water level. Environ.Monit. Assess. 187, 633.

Ferber, L.R., Levine, S.N., Lini, A., Livingston, G.P., 2004. Do cyanobacteria dominate in eutrophic lakes because they fix atmospheric nitrogen? Freshw. Biol. 49, 690–708.

Ger, K.A., Teh, S.J., Goldman, C.R., 2009. Microcystin-LR toxicity on dominant copepods *Eurytemora affinis* and *Pseudodiaptomus forbesi* of the upper San Francisco Estuary. Sci. Total Environ. 407, 4852–4857.

Ger, K.A., Teh, S.J., Baxa, D.V., Lesmeister, S.H., Goldman, C.R., 2010. The effects of dietary Microcystis aeruginosa and microcystin on the copepods of the upper San Francisco Estuary. Freshw. Biol. 55, 1548–1559.

Ha, K., Cho, E., Kim, H., Joo, G., 1999. *Microcystis* bloom formation in the lower Nakdong River, South Korea, importance of hydrodynamics and nutrient loading. Mar. Freshw. Res. 50, 89–94.

International Panel on Climate Change (IPCC), 2007. Climate Change 2007, The Scientific Basis. Contribution of Working Group I to the Fourth Assessment Report of the Intergovernmental Panel on Climate Change. Cambridge University Press New York, NY, USA.

Ibelings, B.W., Havens, K.E., 2008. Cyanobacterial toxins, a qualitative meta-analysis of concentrations, dosage and effects in freshwater estuarine and marine biota. Cyanobacterial harmful algal blooms, state of the science and research needs. Adv. Exp. Med. Biol. 619, 675–732.

Imai, H., Chang, K., Kusaba, M., Nakano, S., 2009. Temperature-dependent dominance of *Microcystis* (Cyanophyceae) species, *M. aeruginosa* and *M. wesenbergii*. J. Plankton Res. 31, 171–178.

International Agency for Research on Cancer, 2006. Carcinogenicity of nitrate, nitrite and cyanobacterial peptide toxins. Lancet Oncol. 7, 628–629.
Jacoby, J.M., Collier, D.C., Welch, E.B., Hardy, F.J., Crayton, M., 2000. Environmental factors associated with a toxic bloom of *Microcystis aeruginosa*. Can. J. Fish. Aquat. Sci. 57, 231–240.
Jassby, A.D., 2008. Phytoplankton in the Upper San Francisco Estuary, Recent biomass trends, their causes and their trophic significance. San Franc. Estuary Watershed Sci. 6 (1) Article 2.
Jiang, Y., Ji, B., Wong, R.N.S., Wong, M.H., 2008. Statistical study on the effects of environmental factors on the growth and microcystins production of bloom-forming cyanobacterium-*Microcystis aeruginosa*. Harmful Algae 7, 127–136.
Jones, J., 2015. California's Most Significant Droughts, Comparing Historical and Recent Conditions. California Department of Water Resources, Sacramento, California, pp. 126. http,//bibpurl.oclc.org/web/74277.
Joung, S., Oh, H., Ko, S., Ahn, C., 2011. Correlations between environmental factors and toxic and non-toxic *Microcystis* dynamics during bloom in Daechung Reservoir, Korea. Harmful Algae 10, 188–193.
Kardinaal, W.E.A., Janse, I., Kamst-van Agterveld, M., Meima, M., Snoek, J., Mur, L.R., Huisman, J., Zwart, G., Visser, P.M., 2007. *Microcystis* genotype succession in relation to microcystin concentrations in freshwater lakes. Aquat. Microb. Ecol. 48, 1–12.
Kim, H.R., Kim, C.K., Ahn, T.S., Yoo, S.A.L., Lee, D.H., 2005. Effects of temperature and light on microcystin synthetase gene transcription in *Microcystis aeruginosa*. Key Eng. Mater. 277–279, 606–611.
Kimmerer, W., 2004. Open water processes of the San Francisco Estuary, From physical forcing to biological responses. San Franc. Estuary and Watershed Sci. 2 (1) article 1.
Kurobe, T., Baxa, D.V., Mion, C.E., Kudela, R.M., Smythe, T.R., Waller, S., Chapman, A. D., Teh, S.J., 2013. Identification of harmful cyanobacteria in the Sacramento-San Joaquin delta and clear lake, California by DNA barcoding. SpringerPlus 2, 491.
Latour, D., Sabido, O., Salencon, M., Giraudet, H., 2004. Dynamics and metabolic acitivity of the benthic cyanobacterium *Microcystis aeruginosa* in the Grangent reservoir (France). J. Plankton Res. 26, 719–726.
Lee, J., Parker, A.E., Wilkerson, F.P., Dugdale, R.C., 2015. Uptake and inhibition kinetics of nitrogen in *Microcystis aeruginosa*: Results from cultures and field assemblages collected in the San Francisco Bay Delta, CA. Harmful Algae 47, 126–140.
Lehman, P.W., Boyer, G., Hall, C., Waller, S., Gehrts, K., 2005. Distribution and toxicity of a new colonial *Microcystis aeruginosa* bloom in the San Francisco Bay Estuary, California. Hydrobiologia 541, 87–90.
Lehman, P.W., Boyer, G., Satchwell, M., Waller, S., 2008. The influence of environmental conditions on the seasonal variation of *Microcystis* abundance and microcystins concentration in San Francisco Estuary. Hydrobiologia 600, 187–204.
Lehman, P.W., Teh, S.J., Boyer, G.L., Nobriga, M., Bass, E., Hogle, C., 2010. Initial impacts of *Microcystis* on the aquatic food web in the San Francisco Estuary. Hydrobiologia 637, 229–248.
Lehman, P.W., Marr, K., Boyer, G.L., Acuna, S., Teh, S.J., 2013. Long-term trends and causal factors associated with *Microcystis* abundance and toxicity in San Francisco Estuary and implications for climate change impacts. Hydrobiologia 718, 141–158.
Lehman, P.W., Kendall, C., Guerin, M.A., Young, M.B., Silva, S.R., Boyer, G.L., Teh, S.J., 2015. Characterization of the *Microcystis* bloom and its nitrogen supply in San Francisco Estuary using stable isotopes. Estuar. Coasts 38, 165–178.
Lehman, P.W., 2004. The Influence of climate on mechanistic pathways that affect lower food web production in Northern San Francisco Bay Estuary. Estuaries 27, 311–324.
Miller, M.A., Kudela, R.M., Mekebri, A., Crane, D., Oates, S.C., Tinker, M.T., Staedler, M., Miller, W.A., Toy-Choutka, S., Dominik, C., Hardin, D., Langlois, G., Murray, M., Ward, K., Jessup, D.A., 2010. Evidence for a novel marine harmful algal bloom, cyanotoxin (microcystin) transfer from land to sea otters. PLoS One 5, e12576.
Mitrovic, S.M., Hardwick, L., Dorani, F., 2011. Use of flow management to mitigate cyanobacterial blooms in the Lower Darling River, Australia. J. Plankton Res. 33, 229–241.
Moisander, P.H., Ochiai, M., Lincoff, A., 2009. Nutrient limitation of *Microcystis aeruginosa* in northern Klamath River reservoirs. Harmful Algae 8, 889–897.
Mosley, L.M., 2015. Drought impacts on the water quality of freshwater systems; review and integration. Earth Sci. Rev. 140, 203–214.
O'Neil, J.M., Davis, T.W., Burford, M.A., Gobler, C.J., 2012. The rise of harmful cyanobacteria blooms: the potential roles of eutrophication and climate change. Harmful Algae 14, 313–334.
Otten, T.G., Paerl, H.W., 2011. Phylogenetic inference of colonly isolates comprising seasonal *Microcystis* blooms in Lake Taihu, China. Microb. Ecol. 62, 907–918.
Otten, T.G., Xu, H., Qin, B., Zhu, G., Paerl, H.W., 2012. Spatiotemporal patterns and ecophysiology of toxigenic *Microcystis* blooms in lake taihu, China, implications for water quality management. Environ. Sci. Technol. 46, 3480–3488.
Paerl, H.W., Huisman, J., 2009. Climate Change. 2009. A catalyst for global expansion of harmful cyanobacterial blooms. Environ. Microbiol. Rep. 1, 27–37.
Paerl, H.W., Otten, T.G., 2013. Harmful cyanobacterial blooms, causes, consequences, and controls. Microb. Ecol. 65, 995–1010.
Paerl, H.W., Paul, V.J., 2012. Climate change, links to global expansion of harmful cyanobacteria. Water Res. 46, 1349–1363.
Paerl, H.W., Scott, J.T., 2010. Throwing fuel on the fire, synergistic effects of excessive nitrogen inputs and global warming on harmful algal blooms. Environ. Sci. Technol. 44, 7756–7758.
Paerl, H.W., Valdes, L.M., Peierls, B.L., Adolf, J.I., Harding Jr., L.W., 2006. Anthropogenic and climatic influences on the eutrophication of large estuarine ecosystems. Limnol. Oceanogr. 51, 448–462.
Paerl, H.W., 1988. Nuisance phytoplankton blooms in coastal, estuarine and inland waters. Limnol. Oceanogr. 33, 823–847.
Rapala, J., Sivonen, K., Lyra, C., Niemela, S.I., 1997. Variation of microcystins cyanobacterial hepatotoxins, in *Anabaena* spp. as a function of growth stimuli. Appl. Environ. Microbiol. 63, 2206–2212.
Redfield, A.C., 1958. The biological control of chemical factors in the environment. Am. Sci. 46, 205–221.
Reynolds, C.S., 1997. Vegetation processes in the pelagic, a model for ecosystem theory. In: Kinne, O. (Ed.), Excellence in Ecology. Ecology Institute, Germany.
Rinta-Kanto, J.M., Ouellette, A.J.A., Boyer, G.L., Twiss, M.R., Bridgeman, T.B., Wilhelm, S.W., 2005. Quantification of toxic Microcystis spp. during the 2003 and 2004 blooms in western Lake Erie using quantitative real-time PCR. Environ. Sci. Technol. 39, 4198–4205.
Robarts, R.D., Zohary, T., 1987. Temperature effects on photosynthetic capacity, respiration, and growth rates of bloom-forming cyanobacteria. N. Z. J. Mar. Freshw. Res. 21, 391–399.
Robson, B.J., Hamilton, D.P., 2003. Summer flow event induces a cyanobacterial bloom in a seasonal Western Australia estuary. Mar. Freshw. Res. 54, 139–151.
Rocha, C., Galvão, H., Barbosa, A., 2002. Role of transient silicon limitation in the development of cyanobacteria blooms in the Guadiana estuary, south-western Iberia. Mar. Ecol. Prog. Ser. 228, 35–45.
SAS Institute, 2013. SAS/STAT User's Guide, Version 8. SAS Institute Inc., SAS Campus Drive, Cary, North Carolina, USA.
Sedmak, B., Eleršek, T., 2006. Microcystins induce morphological and physiological changes in selected representative phytoplankton. Microb. Ecol. 5, 508–515.
Sellner, K.G., Lacouture, R.V., Parlish, K.G., 1988. Effect of increasing salinity on a cyanobacteria bloom in the Potomac River Estuary. J. Plankton Res. 10, 49–61.
Sieracki, C.K., Sieracki, M.E., Yentsch, C.S., 1998. An imaging-in-flow system for automated analysis of marine microplankton. Mar. Ecol. Prog. Ser. 168, 285–296.
Sommer, T.R., Armor, C., Baxter, R., Breuer, R., Brown, L., Chotkowski, M., Culberson, S., Feyrer, F., Gingras, M., Herbold, B., Kimmerer, W., Mueller-solger, A., Nobriga, M., Souza, K., 2007. The collapse of pelagic fishes in the upper San Francisco Estuary. Fisheries 32, 270–277.
Suikkanen, S., Fistarol, G.O., Granéli, E., 2005. Effects of cyanobacterial allelochemicals on a natural plankton community. Mar. Ecol. Prog. Ser. 287, 1–9.
Tsukada, H., Tsujimura, S., Nakahara, H., 2006. Seasonal succession of phytoplankton in Lake Yogo over 2 years, effect of artificial manipulation. Limnology 7, 3–14.
United States Environmental Protection Agency, 1983. Methods for Chemical Analysis of Water and Wastes. Technical Report EPA-600/4-79-020. United States Environmental Protection Agency, Washington, DC, USA.
United States Environmental Protection Agency, 2015 Drinking water health advisory for the cyanobacterial microcystins toxins Technical Report EPA 820R15100. United States Environmental Protection Agency, Washington, DC, USA.
United States Geological Survey, 1985. Methods for Determination of Inorganic Substances in Water and Fluvial Sediments. Open File Report. , pp. 85–495.
Van Gremberghe, I., Leliaert, F., Mergeay, J., Vanormelingen, P., Van der Gucht, K., Debeer, A., Lacerot, G., De Meester, L., Vyverman, W., 2011. Lack of phylogeographic structure in the freshwater cyanobacterium *Microcystis aeruginosa* suggests global dispersal. PLoS One 6, e19561.
Van de Waal, D.B., Verspagen, J.M.H., Lürling, M., Van Donk, E., Visser, P.M., Huisman, J., 2009. The ecological stoichiometry of toxins produced by harmful cyanobacteria, an experimental test of the carbon-nutrient balance hypothesis. Ecol. Lett. 12, 1326–1335.
Vasconcelos, V., Morais, J., Vale, M., 2011. Microcystins and cyanobacteria trends in a 14 year monitoring of a temperate eutrophic reservoir (Aguieira, Portugal). J. Environ. Monit. 13, 668–672.
Verspagen, J.M.H., Passarge, J., Johnk, K.D., Visser, P.M., Peperzak, L., Boers, P., Laanbroek, H.J., Huisman, J., 2006. Water management strategies against toxic Microcystis blooms in the Dutch Delta. Ecol. Appl. 16, 313–327.
World Health Organization, 2011 Guidelines for Drinking-water quality, fourth edition. World Health Organization, Geveva (http,//www.who.int/water_-sanitation_health/publication/2011/dwg_chapter/en/accessed 27 May 014).
Wu, Y., Li, L., Zheng, L., Dai, G., Ma, H., Shan, K., Wu, H., Zhou, Q., Song, L., 2016. Patterns of succession between bloom-forming cyanobacteria *Aphanizomenon flos-aquae* and *Microcystis* and related environmental factors in large, shallow Dianchi Lake, China. Hydrobiologia 756, 1–13.
Xu, H., Paerl, H.W., Qin, B., Zhu, G., Gao, G., 2010. Nitrogen and phosphorus inputs control phytoplankton growth in eutrophic Lake Taihu, China. Limnol. Oceanogr. 55, 420–432.
Zegura, B., Sedmak, B., Filipi, M., 2003. Microcystin-LR induces oxidative DNA damage in human hepatoma cell line HepG2. Toxicon 41, 41–48.
Zilliges, Y., Kehr, J.-C., Meissner, S., Ishida, K., Mikkat, S., Hagemann, M., Kaplan, A., Borner, T., Dittmann, E., 2011. The cyanobacterial hepatotoxin microcystin binds to proteins and increases the fitness of *Microcystis* under oxidative stress conditions. PLoS One 6, e17615.
Zurawell, R.W., Chen, H., Burke, J.M., Prepas, E.E., 2005. Hepatotoxic cyanobacteria, a review of the biological importance of microcystins in freshwater environments. J. Toxicol. Environ. Health 8, 1–37.